

AD-A107 671

UNIVERSITY OF SOUTHERN CALIFORNIA LOS ANGELES  
MULTIPHOTON GAS PHASE SPECTROSCOPY.(U)  
JUN 81 J E WESSEL

F/G 7/4

AFOSR-77-3438

UNCLASSIFIED

AFOSR-TR-81-0749

NL

1 OF 1  
40-A  
107671

END

DATE

FILED

1-82

DTIC

AFOSR-TR- 81 -0749

*final*

**LEVEL** *II*



*9*

AD A707 671

**DTIC**  
**ELECTE**  
NOV 20 1981  
**H**



THE AEROSPACE CORPORATION

DTIC FILE COPY

81 11 17

UNCLASSIFIED

SECURITY CLASSIFICATION OF THIS PAGE (When Data Entered)

REPORT DOCUMENTATION PAGE		READ INSTRUCTIONS BEFORE COMPLETING FORM	
1. REPORT NUMBER <b>AFOSR-TR- 81 -0749</b>	2. GOVT ACCESSION NO. <b>AD-A107671</b>	3. RECIPIENT'S CATALOG NUMBER	
4. MULTIPHOTON GAS PHASE SPECTROSCOPY		5. TYPE OF REPORT & PERIOD COVERED Final	
7. AUTHOR(s) John E. Wessel		6. PERFORMING ORG. REPORT NUMBER	
9. PERFORMING ORGANIZATION NAME AND ADDRESS University of Southern California Los Angeles, CA 90007		8. CONTRACT OR GRANT NUMBER(s) AFOSR 77-3438	
11. CONTROLLING OFFICE NAME AND ADDRESS Office of Scientific Research /NC Air Force Systems Command Bolling AFB, D.C. 20332		10. PROGRAM ELEMENT, PROJECT, TASK AREA & WORK UNIT NUMBERS 61102F 2303/A1	
14. MONITORING AGENCY NAME & ADDRESS (if different from Controlling Office)		12. REPORT DATE 8 June 1981	
		13. NUMBER OF PAGES 69	
		15. SECURITY CLASS. (of this report) Unclassified	
		15a. DECLASSIFICATION/DOWNGRADING SCHEDULE	
16. DISTRIBUTION STATEMENT (of this Report) Approved for public release; distribution unlimited.			
17. DISTRIBUTION STATEMENT (of the abstract entered in Block 20, if different from Report)			
18. SUPPLEMENTARY NOTES			
19. KEY WORDS (Continue on reverse side if necessary and identify by block number) Multiphoton Photoionization Two-Photon Photoionization Laser Detection Ultrasensitive Detection			
20. ABSTRACT (Continue on reverse side if necessary and identify by block number) Multiphoton laser spectroscopy has been investigated as a potential method to improve optical detection for large molecular species. Studies were conducted to establish the photophysics and spectroscopy relevant to molecular detection by multiphoton processes. Detection procedures were optimized on the basis of information derived from the spectroscopic investigations. Detection limits of less than $10^5$ molecules/cm <sup>3</sup> were established for naphthalene, a representative aromatic species. This is a one-thousandfold improvement with respect to			

DD FORM 1473  
(FACSIMILE)

UNCLASSIFIED

SECURITY CLASSIFICATION OF THIS PAGE (When Data Entered)

UNCLASSIFIED

SECURITY CLASSIFICATION OF THIS PAGE(When Data Entered)

19. KEY WORDS (Continued)

20. ABSTRACT (Continued)

the most sensitive prior techniques. The new method was applied to gas chromatography, for which spectrally selective detection was demonstrated. In addition a new method of ultrahigh resolution two-wavelength multiphoton photoionization spectroscopy was proposed, and a preliminary demonstration was made for the iodine molecule.

UNCLASSIFIED

SECURITY CLASSIFICATION OF THIS PAGE(When Data Entered)

ADCRU

20 1981

AEROSPACE REPORT NO.  
ATR-81(7718)-1

## Final Report Multiphoton Gas Phase Spectroscopy

Prepared by  
J. E. WESSEL  
Chemistry and Physics Laboratory

8 June 1981

Prepared for  
UNIVERSITY OF SOUTHERN CALIFORNIA  
Los Angeles, Calif. 90007

Grant No. AFOSR 77-3438

AIR FORCE OFFICE OF SCIENTIFIC RESEARCH (AFOSR)

Contract No. F49620-77-1-0001  
Task Order No. 12-12.

Contract Information Division



Laboratory Operations  
THE AEROSPACE CORPORATION

SECONDARY DISTRIBUTION OF THIS DOCUMENT IS NOT PERMITTED.

## LABORATORY OPERATIONS

The Laboratory Operations of The Aerospace Corporation is conducting experimental and theoretical investigations necessary for the evaluation and application of scientific advances to new military concepts and systems. Versatility and flexibility have been developed to a high degree by the laboratory personnel in dealing with the many problems encountered in the Nation's rapidly developing space systems. Expertise in the latest scientific developments is vital to the accomplishment of tasks related to these problems. The laboratories that contribute to this research are:

Aerophysics Laboratory: Aerodynamics; fluid dynamics; plasmadynamics; chemical kinetics; engineering mechanics; flight dynamics; heat transfer; high-power gas lasers, continuous and pulsed, IR, visible, UV; laser physics; laser resonator optics; laser effects and countermeasures.

Chemistry and Physics Laboratory: Atmospheric reactions and optical backgrounds; radiative transfer and atmospheric transmission; thermal and state-specific reaction rates in rocket plumes; chemical thermodynamics and propulsion chemistry; laser isotope separation; chemistry and physics of particles; space environmental and contamination effects on spacecraft materials; lubrication; surface chemistry of insulators and conductors; cathode materials; sensor materials and sensor optics; applied laser spectroscopy; atomic frequency standards; pollution and toxic materials monitoring.

Electronics Research Laboratory: Electromagnetic theory and propagation phenomena; microwave and semiconductor devices and integrated circuits; quantum electronics, lasers, and electro-optics; communication sciences, applied electronics, superconducting and electronic device physics; millimeter-wave and far-infrared technology.

Materials Sciences Laboratory: Development of new materials; composite materials; graphite and ceramics; polymeric materials; weapons effects and hardened materials; materials for electronic devices; dimensionally stable materials; chemical and structural analyses; stress corrosion; fatigue of metals.

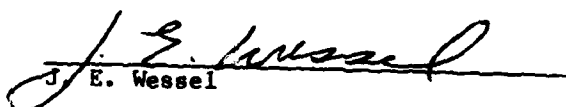
Space Sciences Laboratory: Atmospheric and ionospheric physics, radiation from the atmosphere, density and composition of the atmosphere, aurorae and airglow; magnetospheric physics, cosmic rays, generation and propagation of plasma waves in the magnetosphere; solar physics, x-ray astronomy; the effects of nuclear explosions, magnetic storms, and solar activity on the earth's atmosphere, ionosphere, and magnetosphere; the effects of optical, electromagnetic, and particulate radiations in space on space systems.

Accession	✓
NTIS	
DTIC	
Unannounced	
Justification	
By	
Distribution	
Availability	
Dist	
A	


Report No.  
ATR-81(7718)-1

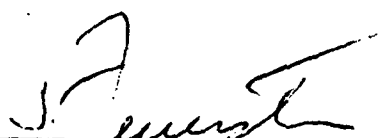
FINAL REPORT:  
MULTIPHOTON GAS PHASE SPECTROSCOPY

Prepared

  
J. E. Wessel

Approved

  
P. F. Jones, Head  
Analytical Sciences Department

  
S. Feuerstein, Director  
Chemistry and Physics Laboratory

## CONTENTS

I.	INTRODUCTION.....	1
II.	DEVELOPMENT OF EXPERIMENTAL METHODS.....	5
III.	DETECTION OF GAS CHROMATOGRAPHY ELUANTS.....	15
IV.	NAPHTHALENE DETECTION LIMIT.....	19
V.	SPECTROSCOPY OF RESONANCE-ENHANCED TWO-PHOTON IONIZATION.....	23
	A. Model for Two-Photon Ionization.....	23
	B. Ambient-Pressure Spectrum.....	25
	C. Low-Pressure Spectrum.....	26
	D. Speculation Concerning Band Shapes.....	33
	E. Saturation Behavior.....	34
	F. Spectroscopic Conclusions.....	34
	REFERENCES .....	35
	BIBLIOGRAPHY.....	37
APPENDICES		
A.	RESONANCE-ENHANCED TWO-PHOTON PHOTOIONIZATION SPECTROSCOPY APPLIED TO DETECTION OF NAPHTHALENE VAPOR.....	A-1
B.	ULTRASENSITIVE DETECTION OF AROMATIC HYDROCARBONS BY TWO-PHOTON PHOTOIONIZATION.....	B-1
C.	GAS CHROMATOGRAPHY WITH DETECTION BY LASER-EXCITED RESONANCE- ENHANCED TWO-PHOTON PHOTOIONIZATION.....	C-1
D.	IONIZATION DIP SPECTROSCOPY: A NEW TECHNIQUE OF MULTIPHOTON IONIZATION SPECTROSCOPY APPLIED TO I <sub>2</sub> .....	D-1



## FIGURES

1.	Schematic Representation of Energy Levels of Naphthalene.....	2
2.	Experimental Apparatus Used for Two-Wavelength Excitation.....	6
3.	Schematic Diagram of the Low-Pressure Ion Detection Cell.....	9
4.	Time-of-Flight-Mass Spectra for Naphthalene.....	10
5.	Saturation Curve for One-Wavelength R2PI Representing Ion Current as a Function of Excitation Pulse Energy.....	12
6.	One-Wavelength R2PI Spectrum of Anthracene Obtained with 5-ns Duration Pulses.....	16
7.	One-Wavelength R2PI Spectrum of Phenanthrene Obtained with 5-ns Duration Pulses.....	17
8.	Naphthalene Vapor Number-Density Measurements.....	22
9.	One-Wavelength R2PI Spectra of Naphthalene.....	24
10.	Comparison of the Low-Pressure and the Ambient Pressure One-Wavelength R2PI Spectra of Naphthalene Presented on a Log Scale Covering the $S_1$ and $S_2$ Regions.....	27
11.	Two-Wavelength Single Vibronic-Level Photoionization Spectra of Naphthalene Obtained at Low Pressure.....	29

## TABLES

1.	Typical Saturation Parameters.....	20
2.	Vibrational Frequencies of Neutral and Cation States of Naphthalene.....	31

## I. INTRODUCTION

There are many scientific and technological problems of interest to the Air Force that require improved optical detection methods. These range from study of potential chemical laser systems to engine monitoring, process control, and environmental monitoring. Until recently, molecular detection methods based on laser-induced fluorescence offered the smallest detection limits for large molecules, namely,  $10^8$  molecules/cm<sup>3</sup>. Advances in resonance-enhanced multiphoton ionization (RMPI) spectroscopy now provide the potential to extend detection capability for large molecules down towards the single-particle limit that has been achieved in atomic detection.<sup>1,2</sup> Conventional one-photon excited molecular fluorescence has three major drawbacks for large molecule detection. (1) Molecular-electronic transitions of complex polyatomic molecules are broad and diffuse. Therefore, the absorption oscillator strength is spread over large spectral regions and the excitation cross sections are reduced correspondingly. (2) The broad transitions lead to poor spectral selectivity. (3) Fluorescence quantum yields are frequently much less than unity.

With these factors in mind, promising multiphoton spectroscopy methods were studied for improved detection. By using resonance-enhanced multiphoton absorption processes with high-intensity laser sources, excitation of each molecule can be achieved even though molecular absorption cross sections are much smaller than those for atoms. By detecting the multiphoton process through the photoionization signal, single ionization events can be observed. Multiple absorption steps provide the possibility of increasing spectral selectivity. In this report we review results from studies of the resonance-enhanced two-photon ionization process (R2PI) applied to detection of large molecules<sup>3-5</sup> (see Fig. 1). The results have demonstrated that the method is applicable to a wide variety of molecular species and that extreme sensitivity can be achieved. Furthermore, it has proven to be highly practical given state-of-the-art tunable laser sources. Aromatic hydrocarbons have been selected for investigation because their spectral properties are ideally

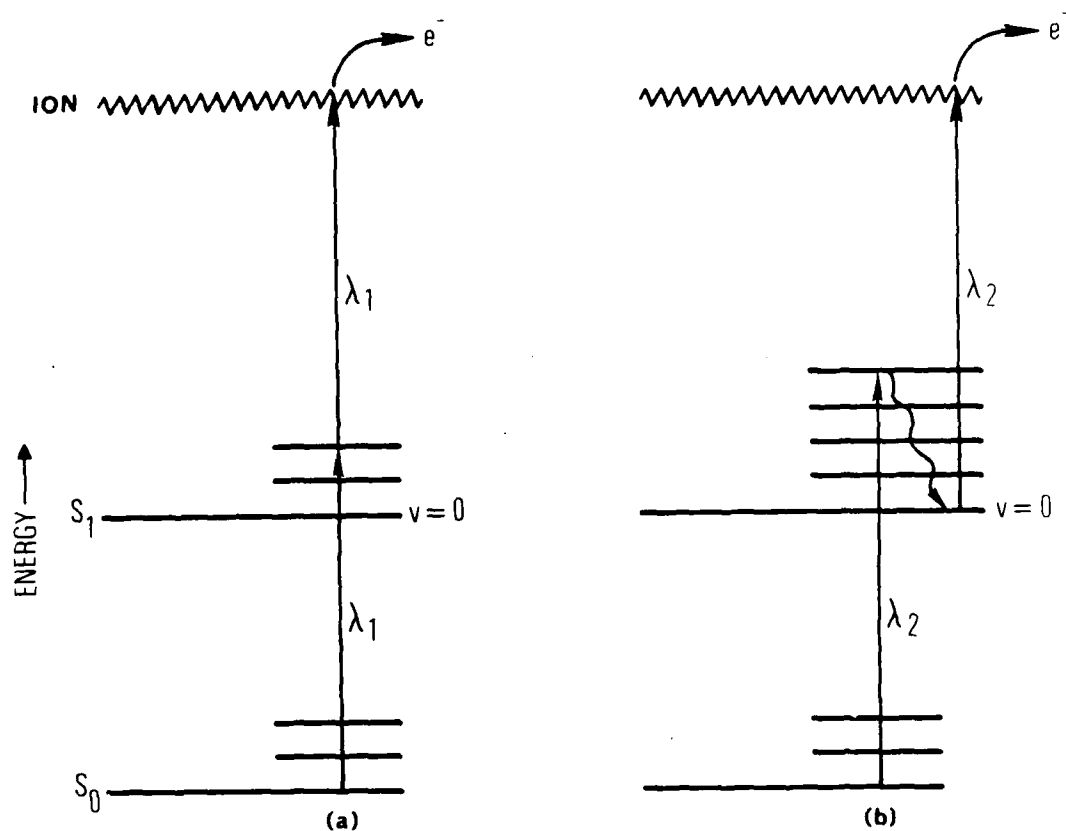


Figure 1. Schematic Representation of Energy Levels of Naphthalene. (a) Direct (low pressure) One-Wavelength. Resonance-Enhanced Two-Photon Ionization (R2PI) with Threshold Wavelength  $\lambda_2$ . (b) Vibrationally Relaxed (ambient pressure) R2PI with Threshold Wavelength  $\lambda_2$ .

matched to available tunable laser sources. In R2PI, one photon excites a strongly allowed electronic transition of the molecule. At low pressure a second photon promotes direct ionization. (At ambient pressure collisions remove vibrational energy in the excited state prior to ionization by the second photon.)

The most important aspects of this program have been described in published reports or will be described in future manuscripts. The published reports are included as Appendices A through D. The first published paper describes the initial demonstration of R2PI applied to naphthalene detection. The other publications describe application of R2PI to gas chromatography, ultrasensitive detection of naphthalene by R2PI, and demonstration of the new two-color high-resolution method of multiphoton ionization spectroscopy that we call ion dip spectroscopy (IDS).

## II. DEVELOPMENT OF EXPERIMENTAL METHODS

Early studies in this program were made using a low-power nitrogen laser pump source. This laser excited one or two dye lasers, each providing energies less than 10  $\mu\text{J}/\text{pulse}$  in the UV with  $10\text{ cm}^{-1}$  linewidth. The 5-ns pulses fluctuated widely in amplitude and in spectral characteristics. Therefore, initial efforts were directed to relatively simple experimental measurements. It was readily established that ionization detection of multiphoton processes is a highly sensitive and practical method. Initial studies were directed to demonstration and characterization of resonance-enhanced two-photon photoionization. Later, greatly improved lasers became available and made possible measurement of high-quality two-photon spectra and accurate determination of detection limits.

The earlier experiments were performed with a single-wavelength excitation source. The more sensitive one-wavelength results were obtained using a high-power Nd:YAG laser with amplifier that pumped a tunable dye laser with amplifier. The frequency of the dye laser was doubled to cover the region from 315 to 220 nm with about 5  $\text{mJ}/\text{pulse}$  and a linewidth of about  $0.1\text{ cm}^{-1}$ . An additional dye laser system was added as a probe source for two-color experiments. It was pumped by about 10% of the Nd:YAG system power, and it provided UV output of about 0.1  $\text{mJ}/\text{pulse}$  with  $0.1\text{ cm}^{-1}$  linewidth. This two-color system is shown in Fig. 2. The major experimental problem encountered in multiphoton spectroscopy using pulsed lasers is caused by pulse-to-pulse fluctuations in intensity, temporal profile, and bandwidth. The first effort to overcome this problem in our work consisted of development of a pulse discriminator system. The measurement is made with a boxcar averager, which samples, holds, and averages data from successive laser pulses. Frequently, laser pulses of abnormal amplitude induced signals 3 to 10 times the size of the average signal. In our experiments, the laser fluctuation is accentuated by factors up to the fourth power because the laser output is frequency doubled and two photons of the doubled output are required for excitation. The fluctuations tend not to average out well over long periods of time.

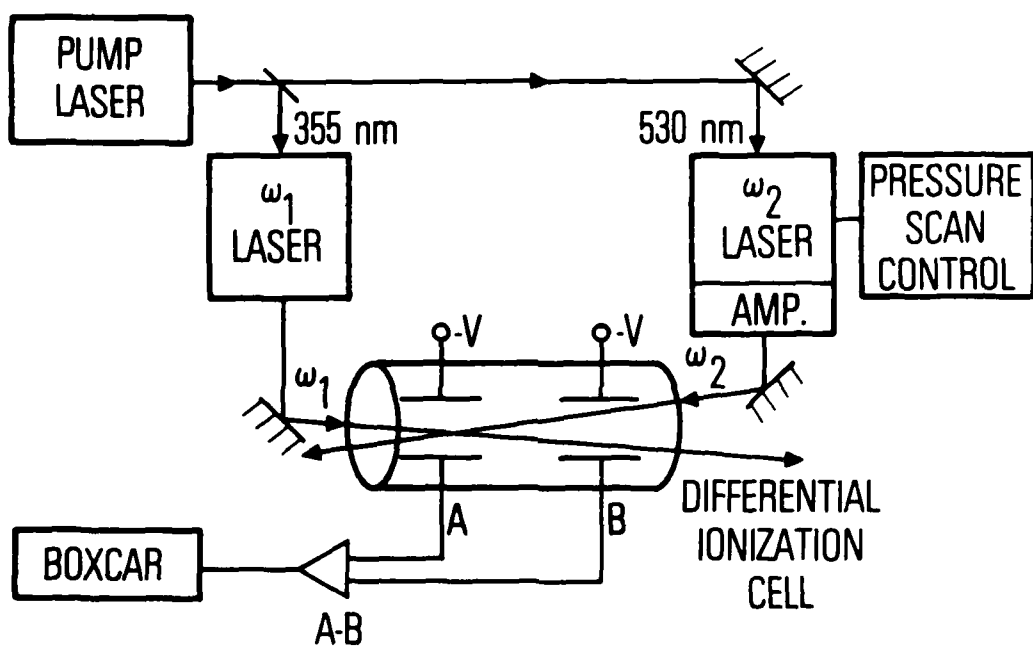


Figure 2. Experimental Apparatus Used for Two-Wavelength Excitation. Differential Detection Provides Output Proportional to the Signal Arising Exclusively from the Combined Effect of Excitation Frequencies  $\omega_1$  plus  $\omega_2$ .

Therefore, a system was set up to reject signals produced by abnormal laser pulses. It was based on a pulse height discriminator, which was activated by a reference signal proportional to laser pulse energy. The discriminator trigger level was set to provide trigger pulses when reference pulses were within a small range of amplitudes. Output pulses were used to trigger the boxcar averager. This reduced the duty cycle by a factor of about 3; however, there was an improvement in signal stability by a factor of about 4 for the same measurement time. The method automatically forced compensation for changes in laser output as a function of wavelength, because it was necessary to adjust the laser pump power to maintain the constant laser output energy that was required to operate the discriminator.

A second aspect of instrumentation for these studies concerns detection of the multiphoton excitation event. Early studies in the program were directed to sensing the process by monitoring fluorescence from the final excited state. For most aromatic molecules, the higher excited states with energy above the first excited singlet state,  $S_1$ , do not fluoresce efficiently. Therefore, special molecules such as azulene, which fluoresces from the  $S_2$  state, were selected for study. It was found that the resonance-enhanced two-photon-excited fluorescence of these molecules was inefficient at the available laser power because of rapid radiationless decay of the intermediate excited state,  $S_1$ . Therefore, emphasis was changed to ionization detection, which proved to be far more suitable for analytical applications.

Ionization detection can be accomplished readily at low pressures by means of an electron multiplier, a Daly detector, a space-charge-limited detector, or a unit gain ionization cell. An electron multiplier was chosen for our work because it provides well-characterized gain, which can be as large as  $10^7$ . An electron multiplier requires pressures below  $\sim 10^{-5}$  Torr. Therefore, the detection system was constructed inside a vacuum system that was subject to continuous pumping. The molecular gas was introduced into the detection system by a needle valve effusive source. Low dark-current background noise was observed when the pressure was substantially less than  $10^{-4}$  Torr. In the presence of laser excitation, a background ion current was present that had temporal characteristics that differed greatly from those for the ion signal

current. This difference probably arises from the time-of-flight associated with the differing paths for ions ejected from cell windows versus molecular ions formed in the focal volume of interest.

The ease in implementing time-of-flight analysis led to studies of multiphoton ionization mass spectrometry. A schematic diagram of the apparatus is shown in Fig. 3. Time-of-flight mass spectra of naphthalene obtained using several excitation intensities are shown in Fig. 4. At low intensities only the parent naphthalene ion ( $C_{10}H_8^+$ ) is formed. At higher intensities extensive fragmentation occurs. These mass spectra provide valuable analytical fingerprints in combination with the optical spectra.

At pressures above ~10 Torr, high-gain detection is readily achieved by using a proportional counter cell. The method proved to be so convenient and reliable that it was used extensively in this program. This is of analytical significance, because ambient pressure measurements are of great practical interest. During the program, a variety of proportional counter devices was constructed that ranged from a 20-cm active region in a 1-m-long ultraclean stainless cell to miniature devices fabricated inside 1/4-in.-diam Swagelok fittings attached to the output port of a gas chromatograph. A high-voltage bias was applied to the central anode wire for the latter configuration. In this case, it was necessary to capacitatively couple the signal in order to block the high-voltage component. The use of a highly stable bias potential (i.e., a stack of batteries) was essential to achieve minimum noise. These problems were avoided in some experiments by constructing cells with a cylindrical negatively biased cathode surrounding the anode wire. Because the more complex design introduced sources of contamination and increased cell volume, it was not used for detection limit studies or for chromatography.

Measurements were performed to characterize current saturation characteristics, voltage dependence of gain, and carrier gas dependence. It was found that all proportional counters saturated as a result of space-charge effects. This was established by comparing signal versus excitation intensity curves at various applied voltages. Departures from quadratic dependence occur at lower intensity when high voltage is applied. This effect is highly pronounced with



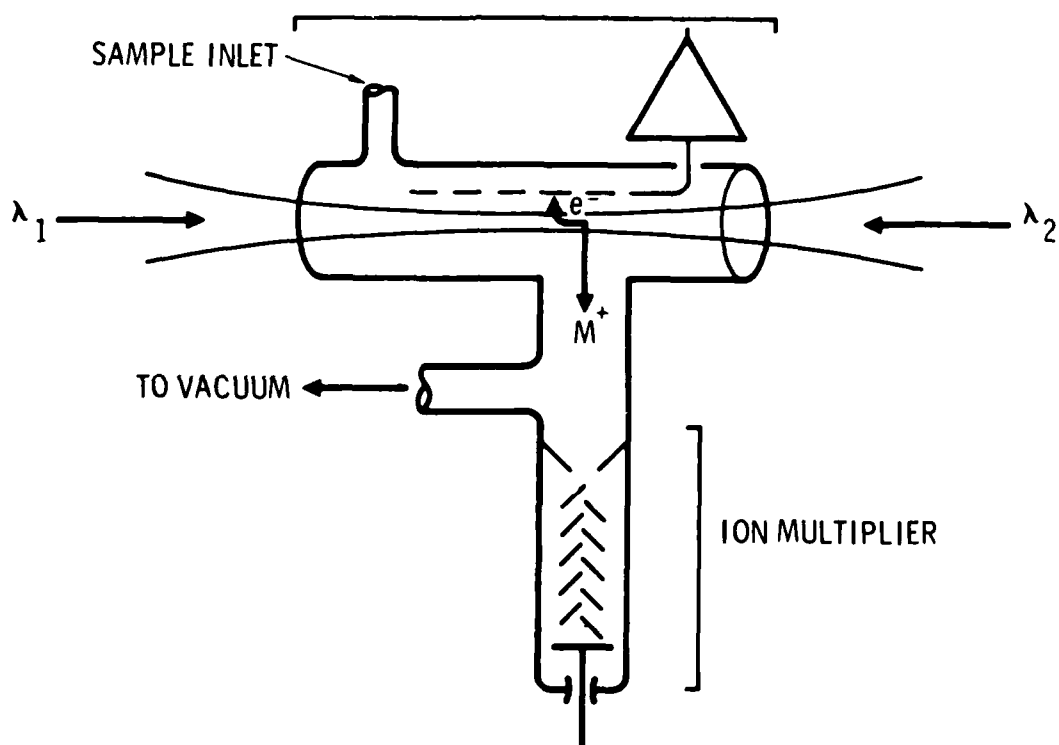


Figure 3. Schematic Diagram of the Low-Pressure Ion Detection Cell. Ions Generated in the Laser Excitation Volume Drift under Uniform Field Conditions to an Ion Multiplier. The Drift Time Depends on the Mass-to-Charge Ratio.

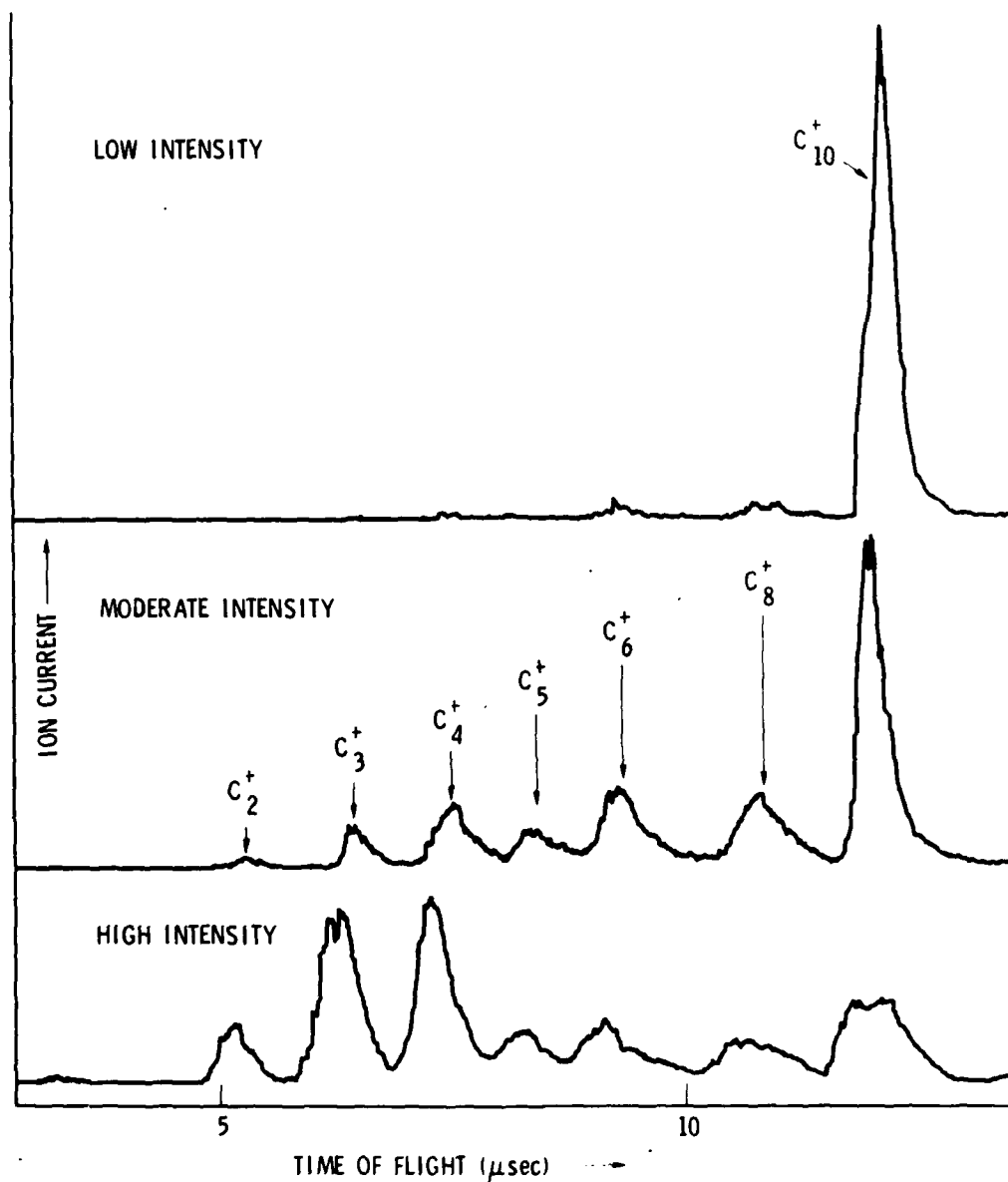


Figure 4. Time-of-Flight-Mass Spectra for Naphthalene. The Mass Resolution is Sufficient to Distinguish Species Differing by One Carbon Atom. At Low Pressures the Parent Ion Dominates, whereas Extensive Fragmentation Occurs at Higher Intensity.

the small proportional counter, which is linear over about three decades at a gain of  $\sim 10^{-4}$ . Larger dynamic ranges were obtained by using a parallel plate unit gain ionization current cell. Many experiments were conducted at unit gain to ensure that a known, temperature-independent response could be obtained. Unit gain operation was confirmed by working in the plateau region of the current-versus-voltage curve. Typically, the plateau is reached at about 5 V applied and extends to 500 or 1000 V before gain exceeds unity.

Optical saturation characteristics were measured by means of a parallel-plate ionization detector. The shape of the optical saturation curves obtained using parallel-plate ionization cells was not changed by reducing the effective excitation volume while maintaining the same excitation intensity. This result confirms that optical saturation occurs. The quadratic dependence of ion current on excitation intensity observed at low intensity (Fig. 5) confirms that two photons are required for ionization of naphthalene. At higher intensity a slope of less than two occurs, indicating that the transition from the ground state ( $S_0$ ) to the first excited state ( $S_1$ ) becomes saturated. At still higher intensity, the slope becomes less than unity, indicating that nearly all interacting molecules are ionized.

For ion detection in nuclear experimentation, P-10 gas, a mixture of 90% argon and 10% methane, is routinely used. The methane prevents secondary ionization events, caused by generation and absorption of vacuum UV radiation, that can result in total gas breakdown. Although there is much work reported in the literature concerning the dependence of proportional counter characteristics on buffer gas composition, we find that for R2PI detection applications, performance is relatively insensitive to composition if the buffer gas is not electronegative. We found that there was little or no practical difference between performance with P-10 gas and pure noble buffer gases such as argon or helium. Gain was greatly decreased with  $N_2$  (down by a factor of  $10^2$  from argon), and only unit gain was obtained for an  $O_2$  buffer. Therefore, a parallel-plate detector with a low-noise preamplifier would be the optimum choice for direct detection in air. State-of-the-art preamplifiers permit detection of about 100 photoelectrons under these circumstances. There is an interesting possibility that simultaneous ion mobility measurements could be

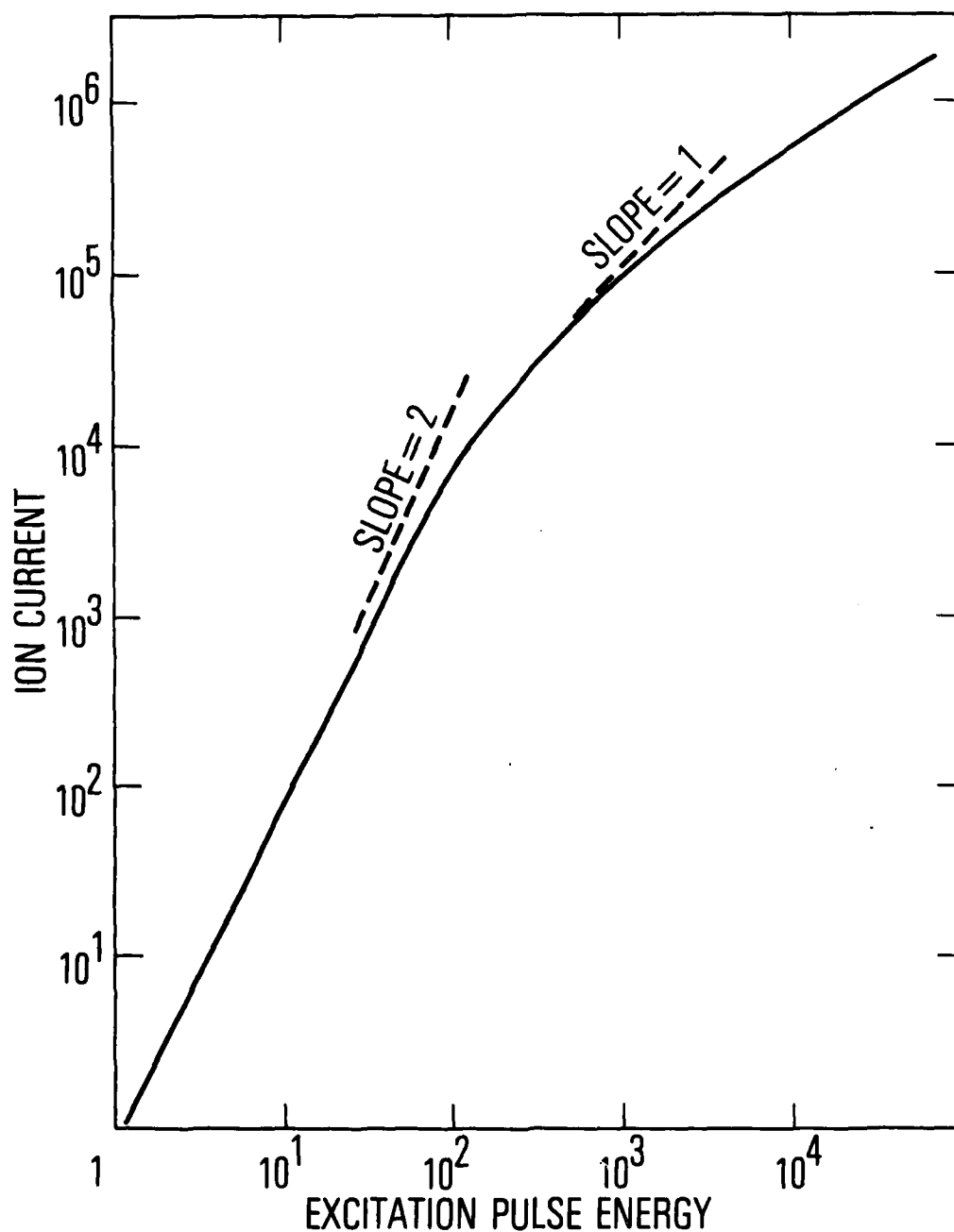


Figure 5. Saturation Curve for One-Wavelength R2PI Representing Ion Current as a Function of Excitation Pulse Energy. Both Scales are Arbitrary and the Highest Intensity Data Correspond to Approximately 0.5 mJ/Pulse in a 1- $\mu$ s Pulse at 279 nm Focused by a 10-cm Lens.

made by modifying the cell and electrodes to provide a uniform field drift region for time-of-flight analysis.

### III. DETECTION OF GAS CHROMATOGRAPHY ELUANTS

On the basis of preliminary considerations, R2PI appeared to be ideally compatible with gas chromatography. At the detector element, the sample is present in a buffer gas that can be chosen to optimize proportional counter performance. The laser beam is readily focused to a volume similar to the dimensions of a chromatograph detector cell. The additional spectral selectivity of R2PI relative to conventional one-photon ionization detectors offers the potential advantage of spectroscopic identification of effluents. Therefore, an effort was made to develop a small volume-proportional counter detection cell and to interface it with a gas chromatograph. (Detailed results are presented in Appendix C.) The available chromatograph was an isothermal instrument with limited performance capability. The laser allocated to the task was of very low power and poor stability. Therefore, the investigations were not directed toward establishing ultimate detection limits or resolution capabilities. Emphasis was on demonstrating that a variety of compounds can be detected by R2PI. Both spectrally selective R2PI detection and multispecies detection were demonstrated. All the aromatic hydrocarbons investigated to date, including naphthalene, benzanthrene, and a series of haloderivatives, were detected with ease and excellent sensitivity.

The method was used for several detailed spectroscopic studies, including a study of the effect of intermediate-state lifetime on detection efficiency. It was found that nearly uniform detection sensitivity could be achieved for the halonaphthalenes by using short-duration excitation pulses, even though the intermediate-state lifetimes decrease drastically from naphthalene (170 ns) to 1-iodonaphthalene ( $\sim 0.5$  ps). The chromatographic detection method was used to measure R2PI spectra for anthracene and phenanthrene. The results are shown in Figs. 6 and 7. For both species, the R2PI onset occurs at the wavelength corresponding to vibrationally relaxed  $S_1$  one-photon ionization. In the case of anthracene, less than 100 collisions can occur during the 10-nsec  $S_1$  lifetime; therefore, vibrational relaxation or vibrational redistribution must be quite efficient.

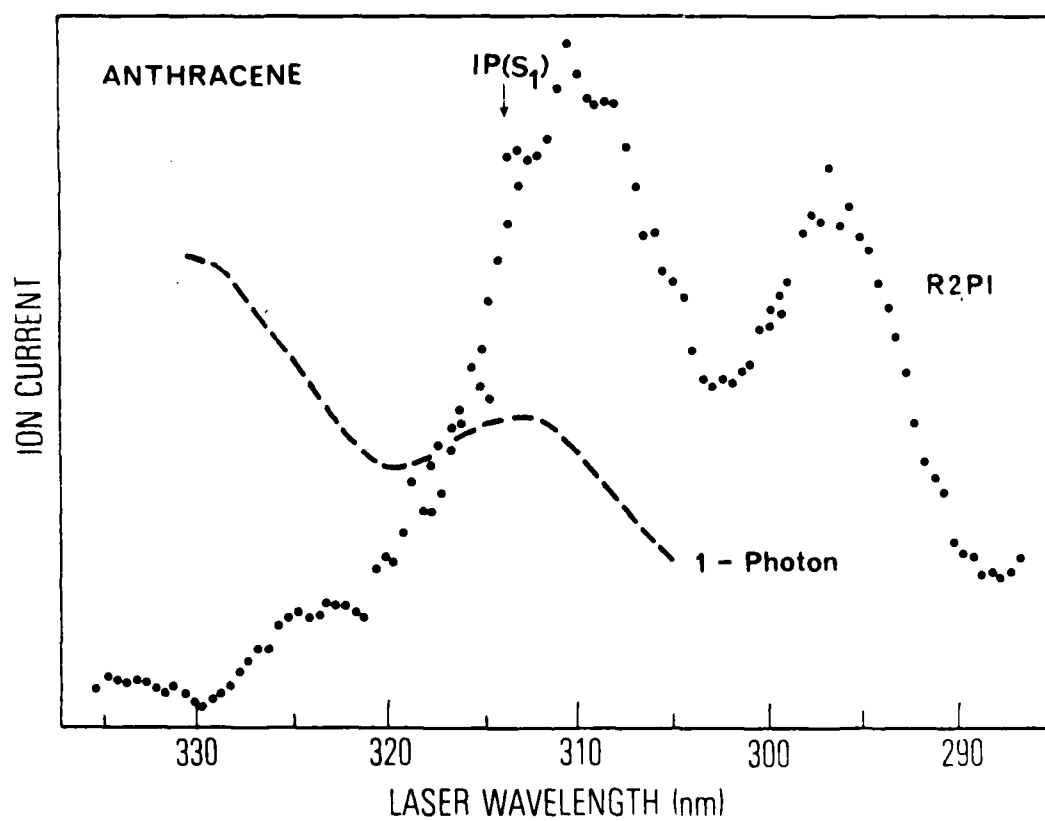


Figure 6. One-Wavelength R2PI Spectrum of Anthracene Obtained with 5-ns Duration Pulses. The Arrow Denotes the Threshold Wavelength for Collisionally Relaxed R2PI and the Dashed Line is the One-Photon Absorption Spectrum.

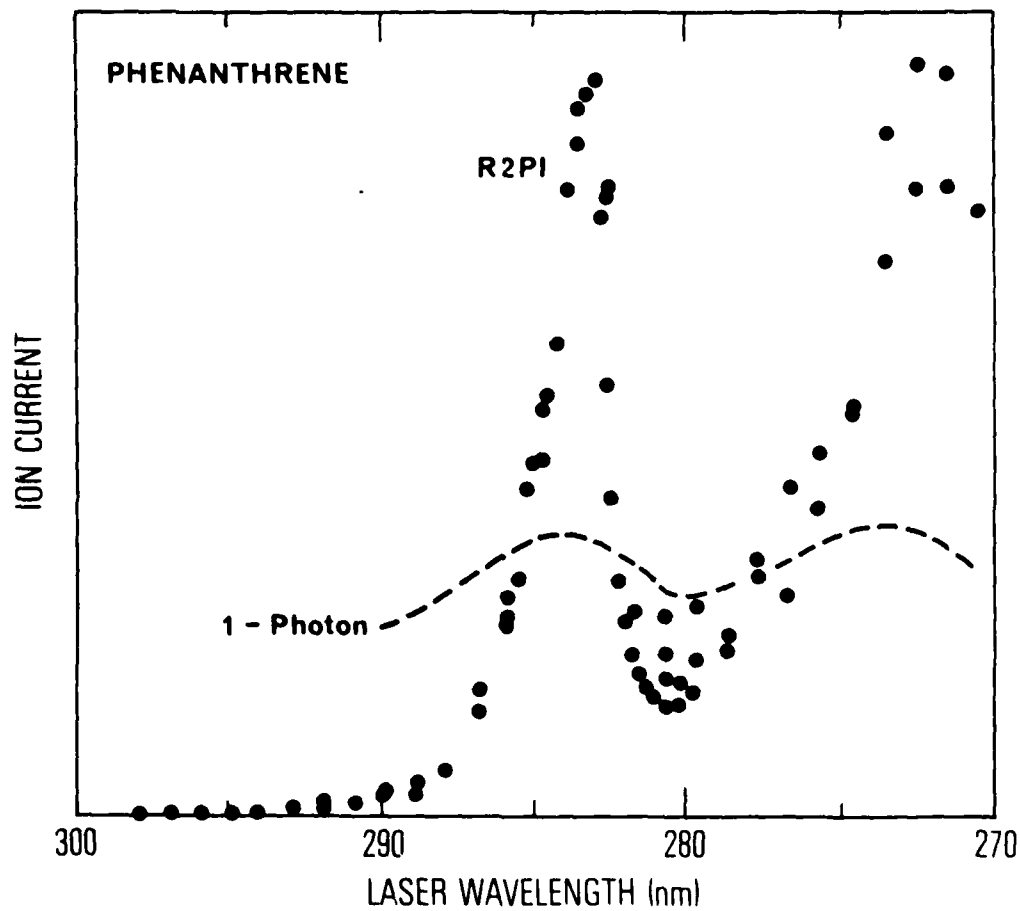


Figure 7. One-Wavelength R2PI Spectrum of Phenanthrene Obtained with 5-ns Duration Pulses. The Arrow Denotes the Threshold Wavelength for Collisionally Relaxed R2PI and the Dashed Line is the One-Photon Absorption Spectrum.



The very crude system used in these studies was demonstrated to have detection limits ( $\sim 10$  pg) comparable to state-of-the-art results for more developed detection methods, such as one-photon photoionization or molecular fluorescence detection. There is no apparent limitation to improving detection by using an improved laser system combined with state-of-the-art gas chromatography. Detection limits of about 1 fg would be anticipated under optimum conditions. It appears the method has real potential for becoming a widely useful analytical tool.

#### IV. NAPHTHALENE DETECTION LIMIT

An experimental system was developed to investigate the ultimate detection limit attainable by R2PI. Results of the investigation are described thoroughly in Appendix C.

Whereas the early experimentation was carried out with low-power lasers that provided pulse energies of 1 to 100  $\mu\text{J}$  in the UV, high-power commercial laser systems were used during the latter part of the program. These new systems were capable of providing 1- to 10-mJ pulses in the UV. The effect of this increased power is easily calculable for the R2PI process. The critical parameter is the maximum laser interaction volume throughout which saturation intensity can be maintained. Therefore, given saturation parameters for molecules of interest, it is possible to calculate the focal volume required to achieve optimum detection.

For a two-photon process excited by a  $\text{TEM}_{00}$  beam, one-half the total signal comes from within the Rayleigh range,  $(16/\pi) (F/d)^2 \lambda$ , where  $F$  is the focal distance,  $d$  is the beam diameter incident on the focusing lens, and  $\lambda$  is the wavelength. The beam maintains a small diameter  $(4/\pi) (F/d) \lambda$  over this distance, and the effective volume of this region is  $64/\pi^2 (f/d)^4 \lambda^3$ . Taking into account the fact that an intensity of  $10^6 \text{ W/cm}^2$  is sufficient to achieve optical saturation for many molecular species of interest, we tabulated in Table 1 the effective excitation volumes possible for various available laser systems.  $\text{TEM}_{00}$  output was assumed. For the low-quality output from the lasers used in these experiments, 10 to 30% of output is effectively in  $\text{TEM}_{00}$ . The remaining higher order modes are far less efficient in inducing multiphoton excitation. The high-power Nd:YAG pumped systems clearly offer superior detection capability. On this basis, the YAG system was chosen for detection limit studies. Naphthalene was selected for study as a representative aromatic hydrocarbon. Extensive spectroscopic information is available for naphthalene, and its vapor pressure and thermodynamic properties have been measured by several research groups. Furthermore, it was known that there are no phase transitions at low temperatures that might interfere with extrapolating

Table 1. Typical Saturation Parameters<sup>a</sup>

	UV Power in TEM <sub>00</sub> (W)	I <sub>s</sub> (W/cm <sup>2</sup> )	Saturated Volume (cm <sup>3</sup> )
Nitrogen-Laser-Pumped Dye Laser	10 <sup>2</sup>	10 <sup>7</sup>	10 <sup>-5</sup>
Flashlamp-Pumped Dye Laser	10	10 <sup>6</sup>	10 <sup>-5</sup>
Nd:YAG-Laser-Pumped Dye Laser	10 <sup>5</sup>	10 <sup>7</sup>	10
CW Dye Laser	1	10 <sup>6</sup>	10 <sup>-7</sup>

<sup>a</sup>These are approximate estimates for the intensity required to ionize most interacting molecules during the laser pulse duration. Estimates are based on the model discussed in the section on spectroscopy of R2PI. It has been assumed that the S<sub>1</sub> + S<sub>0</sub> transition is optically saturated and that the cross section for excited-state ionization controls the ionization rate (appropriate for aromatic hydrocarbons). The intermediate-state ionization cross section is assumed to be 10<sup>-17</sup> cm<sup>2</sup>, and the intermediate-state lifetime is assumed to be longer than the excitation-pulse duration.

vapor pressure curves to the cryogenic temperatures needed to achieve low densities.

A large-volume, ultraclean stainless-steel ionization cell was constructed for the experiments. Naphthalene was introduced into the cell by a flowing carrier gas that passed through a naphthalene vapor generator coil. The entire apparatus was thermostated to maintain a uniform temperature at which the equilibrium vapor pressure would be established. The R2PI signal was recorded as a function of temperature and results from various runs are plotted in Fig. 8. Extensive effort was expended to establish that the signal was directly proportional to the naphthalene number density over the range studied. The measured curve was then joined to higher pressure absolute measurements made by capacitance manometry. Although the results disagree with fairly old vapor pressure data recommended by the National Bureau of Standards, they are fit exceptionally well by a thermodynamic extrapolation (Clausius-Clapeyron equation) using the calorimetrically measured heat of vaporization and heat capacity data. At the detection limit (signal-to-noise ratio = 2) the naphthalene density was  $5 \times 10^4$  molecules/cm<sup>3</sup>, which represents one part naphthalene in  $10^{15}$  parts nitrogen. These studies did not reveal a fundamental limit to obtaining lower detection limits. It appears feasible to extend detection to approximately 10 molecules/cm<sup>3</sup> by using an improved proportional counter or improved preamplifier system combined with a higher power laser of increased spectral bandwidth or increased pulse duration. Extension to other aromatic hydrocarbons with similar ultimate detection limits appears to be readily attainable. The results represent an improvement by a factor of 1000 with respect to the best detection limits that have been obtained for aromatic molecules by other high-sensitivity methods, such as laser fluorescence.

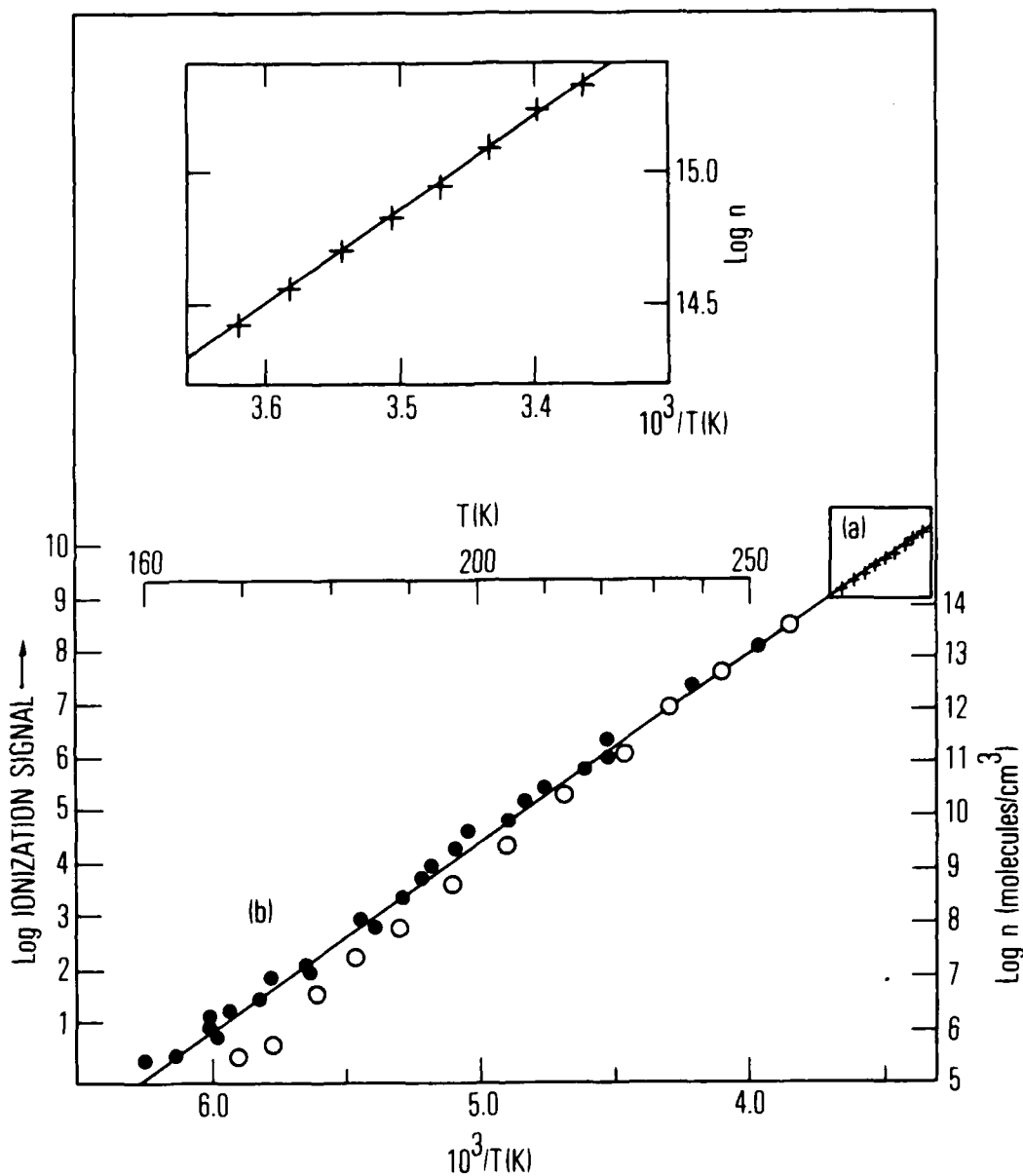


Figure 8. Naphthalene Vapor Number-Density Measurements. (a) Number Densities Deduced from Capacitance Manometer Pressure Measurements. (b) Ionization Signals and Number of Densities Derived from Low-Temperature Ionization Cell Measurements are Displayed as Solid Dots and for Room-Temperature Ionization Cell Measurements by Open Circles. A Solid Line Represents the Theoretical Vapor Pressure Calculated from Calorimetric Data.

## V. SPECTROSCOPY OF RESONANCE-ENHANCED TWO-PHOTON IONIZATION

Multiphoton excitation processes are considerably more complex than conventional one-photon processes. It is essential to develop a detailed understanding of the new spectroscopy in order to use the processes reliably for optical detection applications. Temporal, spectral, and spatial characteristics of the excitation source have a far greater influence on the rates and pathways of multiphoton processes than occurs for one-photon methods, because there is a higher power dependence on instantaneous spectral brightness for multiphoton process. Furthermore, molecular characteristics such as excited-state relaxation processes play roles that differ in multiphoton processes from those in their one-photon counterpart. Therefore, a major fraction of program effort has been devoted to a fundamental study of the relevant processes. The R2PI process was selected as the starting point for investigation because it is the simplest promising multiphoton detection method. Naphthalene was selected for study because it is representative of large aromatic hydrocarbon species and its spectroscopic properties are well known.

### A. MODEL FOR TWO-PHOTON IONIZATION

Our first efforts consisted of obtaining simple one-color two-photon ionization spectra for naphthalene under ambient and low-pressure conditions (Fig. 9). Subsequent work was directed to elucidation of the excitation process. The results are best described by a simple model for the rate (R) of the ionization process summarized in Eq. (1).

$$R = I_{I+K} (\omega_2) \sigma_{I+K} t_K I_{K+O} (\omega_1) \sigma_{K+O} \quad (1)$$

$$t_K = [1/\tau_K + I_{I+K} (\omega_2) \sigma_{I+K} + I_{K+O} (\omega_1) \sigma_{K+O}]^{-1}$$

In these expressions I is the excitation intensity at frequency  $\omega$ ,  $\sigma$  is the cross section,  $t$  is an effective lifetime,  $\tau$  is the natural lifetime, and subscripts O, K, and I specify the ground, intermediate, and ion states, respectively. [Although Eq. (1) is derived using conventional rate equations

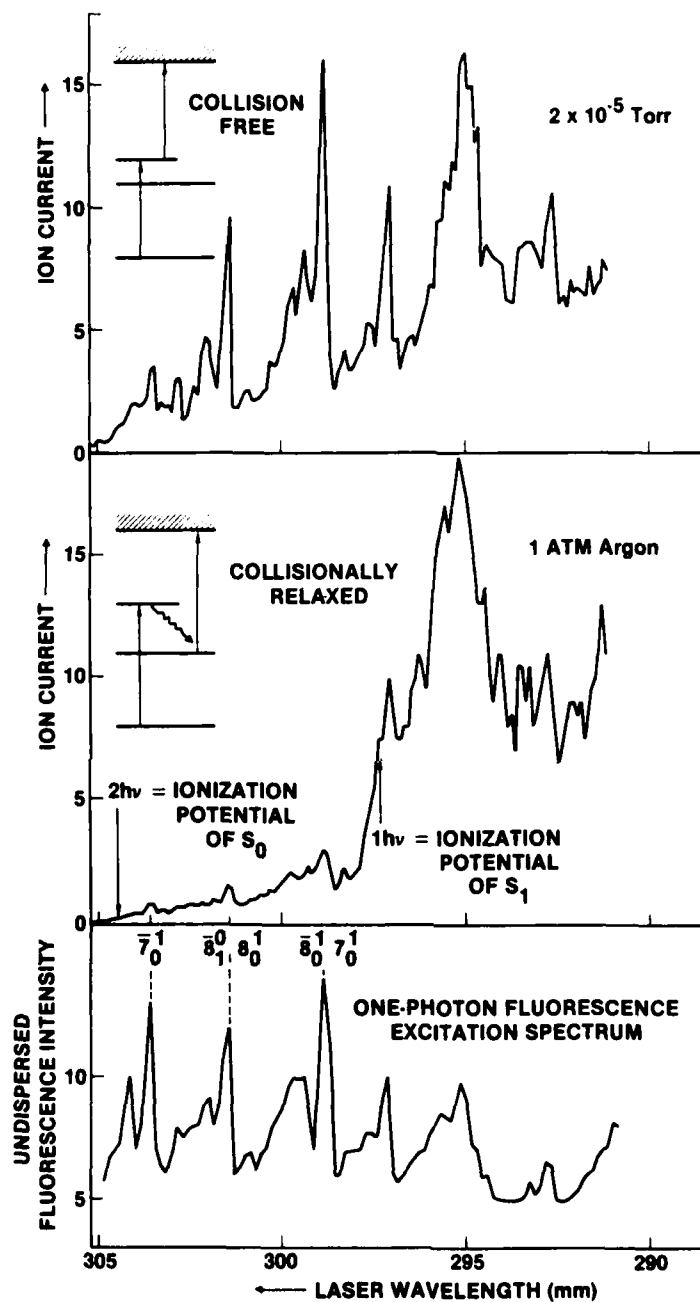


Figure 9. One-Wavelength R2PI Spectra of Naphthalene at Low Pressure and in an Argon Buffer Gas Are Compared with the One-Photon Fluorescence Excitation Spectrum.

that are not generally appropriate for coherent excitation, it has been shown to be valid in this specific situation, provided the ionization rate  $I_{I+0} \sigma_{I+0}$  exceeds the rate  $I_{K+0} \sigma_{K+0}$ . It is also a valid description in the presence of rapid buffer-gas collisions.]

Equation (1) describes a two-step process in which intermediate-state K is populated at a rate  $I_{K0} \sigma_{K0}$ , corresponding to normal one-photon absorption. State K persists for an effective lifetime  $T_K$ , during which interaction with a second photon occurs at a rate given by  $I_{I+K} \sigma_{I+K}$ . This corresponds to one-photon ionization of state K. When a single wavelength source is scanned over the R2PI excitation spectrum, different intermediate states (K) are populated at each different wavelength. Given low-pressure collision-free conditions, the lifetimes and ionization spectra observed from these different levels will differ appreciably. No ionization can occur when the total two-photon energy is less than the ionization energy. Provided there exist substantial off-diagonal matrix elements connecting the intermediate-state K to the ion zero-point level (i.e., nondiagonal Franck-Condon factors), onset of ionization should occur when the threshold condition is satisfied. The literature value for the ionization potential of naphthalene is 8.14 eV, implying an onset wavelength of 304.6 nm.

The observed low-pressure R2PI spectrum is presented in Fig. 9. It has an onset at the expected wavelength and resembles the one-photon absorption spectrum at short wavelengths. The prominent features of the spectrum can be identified in terms of the optically active vibrational modes of  $a_g$  and  $b_{1g}$  symmetry that are seen in the one-photon spectrum. A more detailed discussion of the low-pressure spectrum follows the description of the easily interpreted ambient pressure spectrum.

#### B. AMBIENT-PRESSURE SPECTRUM

At one-atmosphere pressure approximately  $10^{10}$  hard-sphere collisions occur per second. Estimates of  $\sigma_{I+K}$  range between  $10^{-16}$  and  $10^{-18}$  cm<sup>2</sup>; therefore, the ionization rate is about  $10^8$  s<sup>-1</sup> at the intensities used in a typical experiment ( $I \sim 10^{25}$  photons/cm<sup>2</sup> s). This leads to the expectation that vibrational equilibration occurs in the intermediate state prior to



ionization. (The vibrationally equilibrated intermediate-state lifetime of naphthalene in the  $S_1$  state is 170 ns at 298 K in an argon buffer gas.) Collisions remove any excess vibrational energy imparted by the first photon, thereby shifting the onset wavelength to the blue. This effect is evident in the ambient-pressure spectrum of Fig. 9.

Rapid collisional equilibration leads to a simple model for the R2PI spectrum, in which the effective intermediate state has a uniform lifetime regardless of excitation wavelength. Furthermore, the effective  $S_1$  photoionization spectrum becomes independent of the first photon wavelength. This should provide a major simplification because the  $S_1$  ionization spectrum should resemble a simple step function, i.e., zero for photons with energy less than the  $S_1$  ionization potential. The ionization rate should rise abruptly to a plateau above the  $S_1$  ionization threshold. Thus, relaxation can be incorporated into Eq. (1) by using a new effective lifetime and a relaxed ionization spectrum to describe  $\sigma_{I+K}$ . The ambient-pressure R2PI spectrum should closely resemble the one-photon absorption spectrum at photon energies in excess of the  $S_1$  ionization threshold, provided the  $S_1$  ionization cross section is independent of wavelength in the region of interest above the threshold (this is the case for atoms, as has been proven by Wigner). This expectation is justified by the ambient-pressure spectrum of Fig. 10, which closely resembles the one-photon absorption spectrum for  $\lambda < 297$  nm. In fact, the  $S_1$  ionization spectrum can be extracted from the low-pressure R2PI spectrum by dividing the R2PI spectrum by the one-photon absorption spectrum. In summary, the ambient pressure R2PI spectrum is readily explained by a simple two-step excitation model.

### C. LOW-PRESSURE SPECTRUM

Interpretation of the low-pressure spectrum is somewhat more complex because each intermediate vibronic state has a different ionization spectrum and different rate parameters. If there were no nuclear geometry change and no frequency change between the  $S_1$  state and the ionized state, and if the electronic and vibrational wavefunctions of the two states were separable into individual product terms, then the one-photon ionization spectra for different

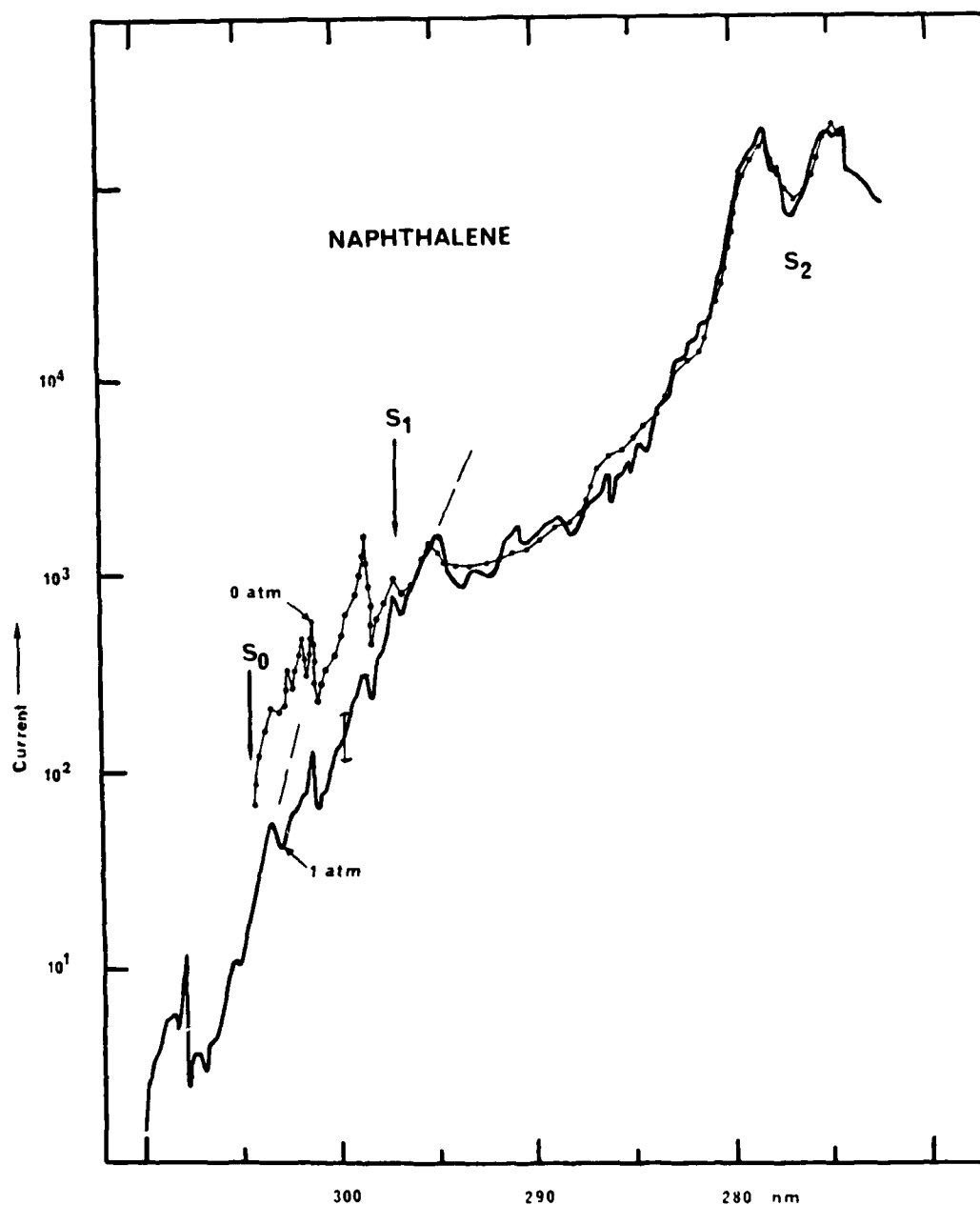


Figure 10. Comparison of the Low-Pressure and the Ambient Pressure One-Wavelength R2PI Spectra of Naphthalene Presented on a Log Scale Covering the  $S_1$  and  $S_2$  Regions. The Arrow  $S_0$  Denotes the Theoretical Threshold Wavelength for Two-Photon Ionization from  $S_0$ , whereas the Arrow Labeled  $S_1$  Denotes the Wavelength Required for Ionization from Vibrationally Relaxed  $S_1$  Naphthalene.  $S_2$  is the Region of the Second Strong One-Photon Transition.

intermediate states would be the same. Assuming uniform rate parameters, the R2PI spectrum would match the ambient-pressure spectrum in Fig. 9.

The observed R2PI spectrum reveals vibronic bands at  $\lambda < 297$  nm in the low-pressure spectrum with intensities nearly ten times those in the ambient-pressure spectrum. These can occur only if large off-diagonal vibrational overlap integrals connecting  $S_1$  with the zero-point level of the ionized state exist. The prominent transitions in this region include (Fig. 10)  $b_{1g}(7)_0^1$  \* at 303.7 nm, which lies at slightly more than half the ground-state ionization energy;  $a_g(8)_0^1 b_{1g}(8)_0^1$  at 301.5 nm, which has a Franck-Condon component (i.e., the  $a_g$  mode change is involved); and  $a_g(7)_0^1 b_{1g}(8)_0^1$  at 299.0 nm, again with a Franck-Condon component. Vibronic coupling in  $S_1$  must induce the first of these transitions because the overlap integral  $\langle 0 \times b_{1g} | 1 \times b_{1g} \rangle$  between any two electronic states vanishes, provided the molecular point group is preserved. Two-color ionization experiments were used to obtain the one-photon single vibronic level (SVL) ionization spectra for  $S_1$  naphthalene. These spectra are shown in Fig. 11. When the  $S_1$  zero-point level is pumped (using the 317-nm hot band transition  $b_{1g}(8)_0^1$ ), a beam of  $\lambda_2$  generates the ionization signal recorded in Fig. 11. It has the expected step function behavior with onset at 297.5 nm. The corresponding ionization energy from the ground state is 8.138 eV, in close agreement with the N.B.S. recommended value of 8.14 eV. The region of shorter wavelength is remarkably devoid of features. Additional steps (increases in signal) are anticipated at intervals corresponding to excitation of  $a_g$  (and perhaps  $b_{1g}$ ) modes in the ion; however, they are not evident. It is presumed that they are of small amplitude ( $< 2\times$  increase in signal) and thus masked by the appreciable noise level (a log scale is used to present the data). The masked steps may account for the general rise of ionization signal to shorter wavelength.

\*The notation  $a_g(X)_0^1 b_{1g}(Y)_0^1$  designates the transition between the zero-point level in the lower energy state and the combination mode in the upper state consisting of one quantum in totally symmetric mode number X and one quantum in the number Y mode of  $b_{1g}$  symmetry.

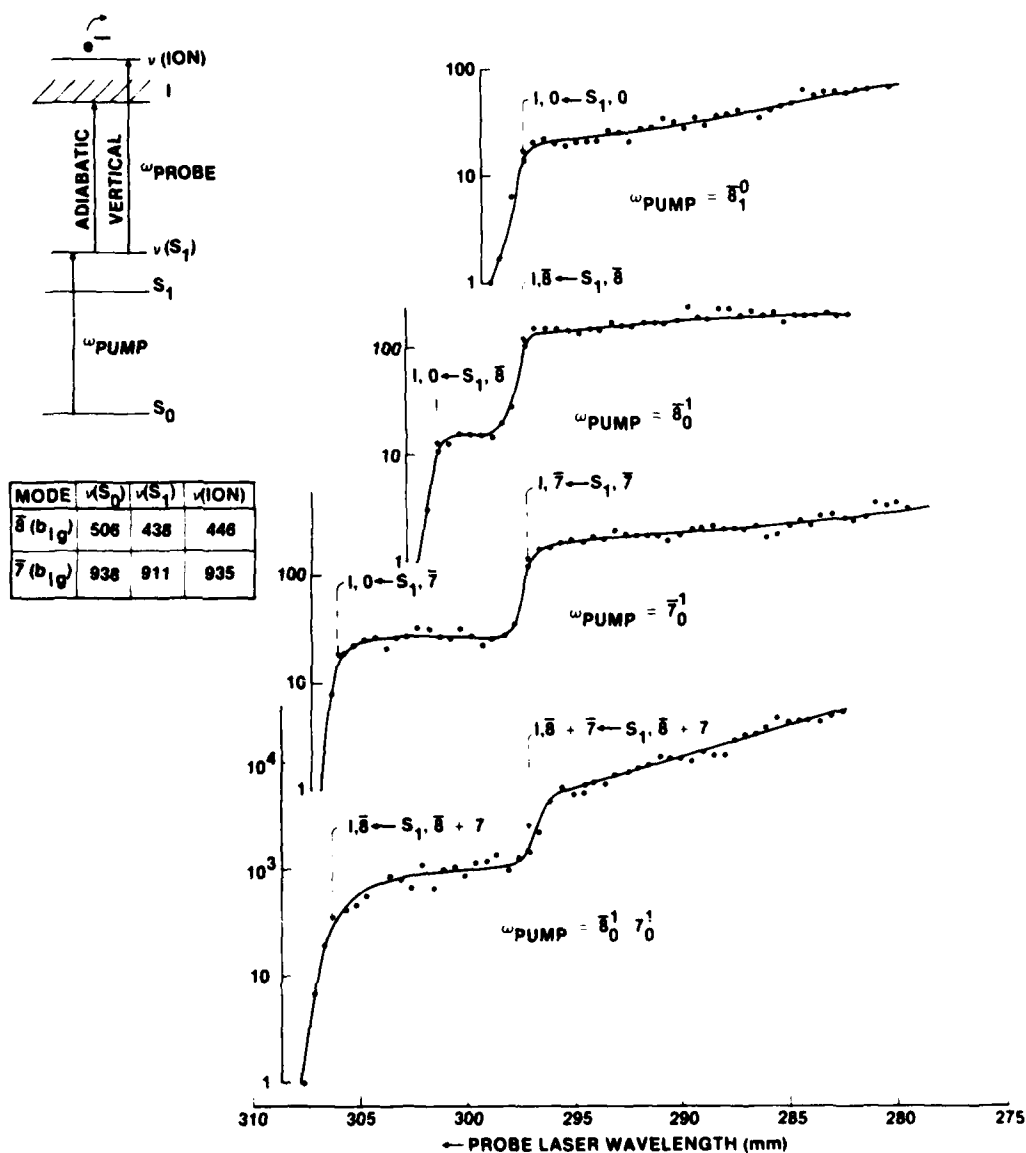


Figure 11. Two-Wavelength Single Vibronic-Level Photoionization Spectra of Naphthalene Obtained at Low Pressure. Various Intermediate States are Prepared by Choosing an Appropriate Pump Wavelength. The Spectra Display the Ion Current as a Function of the Probe Wavelength. ( $\bar{8}$  and  $\bar{7}$  designate vibrational modes of  $b_{1g}$  symmetry, whereas  $\bar{7}$  refers to a mode of  $a_g$  symmetry.)

Absence of intense discrete transitions to Rydberg states near the ionization potential and the absence of autoionizing resonances above it is of considerable interest. If this type of structure were present it could provide useful additional selectivity. Further searches for these transitions in naphthalene and other molecules are clearly warranted.

Multiple-onset steps are present in low-pressure spectra recorded for various intermediate states (Fig. 11). When  $\lambda_1$  was selected to excite  $b_{1g}(8)_0^1$ , the first ionization step was located at 301.2 nm, corresponding to the transition  $I, 0 \leftarrow S_1, b_{1g}(8)$  which is offset from the larger step that corresponds to  $I, b_{1g}(8) \leftarrow S_1, b_{1g}(8)$  by  $446 \text{ cm}^{-1}$ . The wavelength for the latter step implies that the  $b_{1g}(8)$  fundamental is  $446 \text{ cm}^{-1}$  in the ionized state. The first (off-diagonal) transition has an amplitude about one-tenth of the diagonal transition. This corresponds closely to the known magnitude of vibronic mixing in the  $S_1$  state induced by  $b_{1g}(8)$ . [The  $b_{1g}(8)$  mode mixes zero-point  $B_{2u}(S_2)$  amplitude into the  $B_{3u}(S_1)$  state. This is well documented in the one-photon spectrum. Therefore, the transition from  $b_{1g}(8)$  can terminate on the zero-point level of the ion, even though there is zero overlap for the  $b_{1g}(8)$  mode.]

Similar behavior is observed for  $b_{1g}(7)$  and for the combination  $b_{1g}(8) + a_g(7)$ . In the latter case the off-diagonal transition corresponds to  $b_{1g}(8) \leftarrow S_1, b_{1g}(8) a_g(7)$ , and it has an intensity about one-quarter that for the vertical transition. In Table 2 vibrational frequencies calculated for the ion are compared with frequencies in the ground and  $S_1$  states. Values for the ion are intermediate between those for the two bound states, presumably reflecting promotion of the optical electron from a bonding to antibonding orbital (in  $S_1$ ) and to a nonbonding configuration in the ion.

The Franck-Condon factors derived from the spectra recorded in Fig. 11 can be used to predict the appropriate factors for one-color R2PI transitions. The intensities predicted for transitions with  $\lambda < 297 \text{ nm}$  are low relative to the measured spectrum, which accurately coincides with the intensities for the relaxed ambient-pressure spectrum. The tentative explanation is that vibrational redistribution occurs in  $S_1$  vibronic levels excited by  $\lambda < 297 \text{ nm}$ .

Table 2. Vibrational Frequencies of Neutral and Cation States of Naphthalene

Mode	State (cm <sup>-1</sup> )		
	S <sub>0</sub>	S <sub>1</sub>	Ion <sup>a</sup>
$\bar{8}^b$	506	438	450
$\bar{7}^b$	938	911	930
7 <sup>b</sup>	1020	987	1030

<sup>a</sup>This work. Experimental error estimated to be  $\pm 10$  cm<sup>-1</sup>.  
<sup>b</sup> $\bar{8}$  and  $\bar{7}$  designate vibrational modes of b<sub>1g</sub> symmetry, whereas 7 refers to a mode of a<sub>g</sub> symmetry.

This results in a scrambling of modes. The mixed modes are predominately of low-energy nontotally symmetric character. They have no off-diagonal overlap integrals; therefore, their transitions to the ion are diagonal and occur very near the 0-0 transition (297 nm). The close match between low-pressure and ambient-pressure one-color R2PI spectra for  $\lambda < 297$  nm implies that vibrational redistribution occurs on a time scale shorter than the 5-ns duration of the probe pulse for S<sub>1</sub> states with 1600 cm<sup>-1</sup> or more vibrational energy.

#### D. SPECULATION CONCERNING BAND SHAPES

It is interesting to speculate concerning the reason for the observed differences in vibronic band shapes of the low- and ambient-pressure spectra in the region 304 to 297 nm. Even at low resolution, the R2PI band shapes differ substantially from the one-photon band shapes. Consider the prominent 301.5-nm band corresponding to excitation of a<sub>g</sub>(8)<sub>0</sub><sup>1</sup> b<sub>1g</sub>(8)<sub>0</sub><sup>1</sup>. In the ambient-pressure R2PI spectrum, there is much less intensity on the low-energy shoulder. (In the one-photon absorption spectrum, the shoulder derives most of its intensity from sequence bands.) This can be explained in that extra thermal

energy imparted to the intermediate state by sequence excitation is lost by collisional relaxation at ambient pressure. The slightly higher energy available on the blue edge of the band should excite hot-band transitions from the relaxed  $S_1$  state more effectively; therefore, the sequence bands on the red edge should be less prominent. The effect is dramatic in the case of  $b_{1g}(7)_0^1$  at 304 nm for which the sequence structure nearly vanishes. This suggests that a more prominent sequence shoulder at 302 nm for  $a_g(8)_0^1 b_{1g}(8)_0^1$  may result from unrelaxed R2PI.

In the low-pressure R2PI spectrum, the 301.5-nm band corresponding to  $a_g(8)_0^1 b_{1g}(8)_0^1$  has a prominent sequence structure that can be attributed to absence of vibrational redistribution in the intermediate-excited state. Although the main band at 299 nm corresponding to  $a_g(7)_0^1 b_{1g}(8)_0^1$  has similar intensification with respect to the ambient-pressure spectrum, sequence features of this band are greatly suppressed. The effect presumably arises from vibrational redistribution in the higher energy intermediate states involved in sequence excitation. This implies that collisionless redistribution becomes efficient for  $1600\text{ cm}^{-1}$  excess vibrational energy in  $S_1$  [in the mode corresponding to  $a_g(7)_0^1 b_{1g}(8)_0^1 X_n^n$  (sequence)]. The structure at 301.5 nm implies that redistribution is inefficient at  $1300\text{ cm}^{-1}$ , corresponding to  $a_g(8)_0^1 b_{1g}(8)_0^1 X_1^1$ .

In the very-low-energy region (308 nm), a low-intensity feature has been recorded corresponding to  $b_{1g}(8)_0^1$ . This is a hot band involving thermal excitation in  $S_1$  at slightly higher energy (305 nm). There is a hot-band feature that can be explained by unrelaxed two-photon absorption from  $a_g(9)$  at  $516\text{ cm}^{-1}$  in the ground state.

#### E. SATURATION BEHAVIOR

The saturation curve for R2PI, in which ion current is plotted versus laser pulse energy, contains significant information with respect to dynamics of the excitation process. Simple models of the rate processes made for low-intensity short-duration or long-duration excitation pulses lead to expectations of quadratic intensity dependence. This behavior is confirmed for 1- $\mu\text{sec}$  duration excitation pulses at 278 nm, corresponding to  $S_2$  excitation. As intensity is increased, it is anticipated that the  $S_2 \rightarrow S_0$  transition will

saturate\* (at  $\sim 2 \times 10^5$  W/cm<sup>2</sup>) for 1- $\mu$ sec excitation pulses based on the known one-photon cross section of  $2 \times 10^{-17}$  cm<sup>2</sup>.

This should cause departure from a slope of 2 at a pulse energy corresponding to  $10^2$  in Fig. 5. The cross section for  $I \rightarrow S_1$  is expected to be in the range  $10^{-17}$  to  $10^{-18}$  cm<sup>2</sup>. Therefore, an intensity of  $\sim 10^6$  W/cm<sup>2</sup> should cause every  $S_1$  molecule to ionize within the 170-ns lifetime of relaxed  $S_1$  naphthalene. The slope in Fig. 5 becomes less than unity at an energy consistent with this intensity. It appears that the data support the assumed  $S_1$  ionization cross section, and the experiments demonstrate that photoionization efficiency can be made to approach unity in the laser interaction volume ( $\sim 10^{-5}$  cm<sup>3</sup> in these experiments).

#### F. SPECTROSCOPIC CONCLUSIONS

From this study of naphthalene vapor, it can be concluded that there are many subtle differences between ambient- and low-pressure R2PI spectra. For most analytical applications the differences will not be highly significant, although quantitative measurements will require appropriate correction for background pressure. These complications can be largely avoided by exciting into the  $S_2$  region; however, there is then some loss in spectral selectivity. It can be anticipated that similar considerations will apply to the detailed spectroscopy of most other aromatic species.

---

\*Saturation, in this context, is a condition of significant departure from low-intensity behavior caused by such factors as ground-state depletion and bottleneck effects in optically inaccessible states.



#### REFERENCES

1. Gelbwachs, J. A., C. F. Klein, and J. E. Wessel, "Single - Atom Detection by SONRES," IEEE J. Quantum Elec. 14, 121-125, 1978.
2. Hurst, G. S., M. H. Nayfeh, and J. P. Young, "A Demonstration of One-Atom Detection," Appl. Phys. Lett. 30, 229-231, 1977; Hurst, G. S.; M. G. Payne, S. D. Kramer, and J. P. Young, "Resonance Ionization Spectroscopy and One-Atom Detection," Rev. Mod. Phys. 51, 767-819, 1979.
3. Frueholz, R., J. E. Wessel, and E. Wheatley, Resonance-Enhanced Two-Photon Photoionization Spectroscopy Applied to Detection of Naphthalene Vapor," Anal. Chem. 52, 281-284, 1980.
4. Klimcak, C. and J. E. Wessel, "Ultrasensitive Detection of Aromatic Hydrocarbons by Two-Photon Photoionization," Appl. Phys. Lett. 37, 138-141, 1980.
5. Klimcak, C. and J. E. Wessel, "Gas Chromatography with Detection by Laser-Excited Resonance-Enhanced 2-Photon Photoionization," Anal. Chem. 52, 1233-1239, 1980.

PRECEDING PAGE BLANK-NOT FILMED

## BIBLIOGRAPHY

### Publications

- Frueholz, R., J. E. Wessel, and E. Wheatley, "Resonance Enhanced Two-Photon Photoionization Spectroscopy Applied to Detection of Naphthalene Vapor," Anal. Chem. 52, 281 (1980).
- Klimcak, C. M., and J. E. Wessel, "Gas Chromatography with Detection by Laser Excited Resonance Enhanced Two-Photon Photoionization," Anal. Chem. 52, 1233 (1980).
- Klimcak, C. M., and J. E. Wessel, "Ultrasensitive Detection of Aromatic Hydrocarbons by Two-Photon Photoionization," Appl. Phys. Lett. 37, 138 (1980).
- Cooper, D. E., C. M. Klimcak, and J. E. Wessel, "Ionization Dip Spectroscopy, A New Technique of Multiphoton, Ionization Spectroscopy Applied to I<sub>2</sub>," Phys. Rev. Lett., 46, 324 (1981).

### Presentations

- Klimcak, C. M., "Resonance Enhanced Two-Photon Photoionization Spectroscopy Applied to Molecular Detection," American Chemical Society National Meeting, Houston, Texas, March 1980 (Invited).
- Wessel, J. E., "Multiphoton Spectroscopy Applied to Trace Molecular Detection," Colorado State University, Fort Collins, Colorado, June 1979 (Invited).
- Wessel, J. E., "Resonance Enhanced Multiphoton Spectroscopy of Naphthalene," Princeton University, Princeton, New Jersey, September 1979 (Invited).
- Wessel, J. E., "Ionization Dip Spectroscopy," International Conference on Quantum Electronics, Boston, Massachusetts, June 1980.
- Klimcak, C. M. and J. E. Wessel, "Intermediate State Vibrational Relaxation in 2-Photon Ionization of Single Vibronic Level Ionization and Naphthalene," National Meeting American Chemical Society, Las Vegas, Nevada, August 1980.

### Manuscripts in Preparation

- Frueholz, R., C. M. Klimcak, J. E. Wessel, and E. Wheatley, "Vibrational Relaxation Processes in S<sub>1</sub> Naphthalene" (journal paper).
- Wessel, J., "Vibrational Overtone Resonance Enhancement in Two-Photon Absorption" (journal paper).

Cooper, D. E., Klimcak, C. M., and Wessel, J. E., "Ultrasensitive Molecular Detection by Multiphoton Ionization Spectroscopy," Proc. Society of Photo-optical Instrumentation Engineers (1981).

APPENDIX A

Resonance Enhanced Two-Photon Photoionization Spectroscopy  
Applied to Detection of Naphthalene Vapor

# Resonance Enhanced Two-Photon Photoionization Spectroscopy Applied to Detection of Naphthalene Vapor

Robert Frueholz, John Wessel,\* and Eric Wheatley<sup>1</sup>

Ivan A. Getting Laboratories, The Aerospace Corporation, P.O. Box 92957, Los Angeles, California 90009

Resonance enhanced two-photon photoionization spectroscopy has been applied to detection of naphthalene vapor in an ambient pressure buffer gas. This new molecular detection method provides spectral selectivity and is potentially applicable to most molecular species. Ionization was monitored with a proportional counter that is capable of responding to creation of a single ion-electron pair. An analytical curve was obtained with a detection limit corresponding to  $<10^7$  molecules/cm<sup>3</sup>. Improved laser sources are expected to improve this detection limit by several orders of magnitude.

Techniques of multiphoton spectroscopy offer the potential to overcome several key problems encountered in optical detection of molecular species at low concentrations. In this report we describe application of resonance enhanced two-photon photoionization (R2PI) to detection of naphthalene vapor in an ambient pressure buffer gas. The excitation processes are shown in Figure 1. Sub-part-per-trillion detection limits were achieved using a low energy (0.2 mJ) pulsed ( $10^{-6}$  s) laser source. The experiments reported here were conducted using a single wavelength from a tunable laser to provide both photons required for the 2-photon excitation. Ion generation was monitored in an ambient pressure buffer gas using a proportional counter detector. Results from the more selective multiple wavelength excitation experiments will be reported at a later time.

Resonance enhanced multiphoton ionization (RMPI) has the potential ability to achieve a detection limit approaching one molecule (in the laser interaction volume). Therefore it is informative to compare the method to fluorescence spectroscopy which is the highest sensitivity conventional method of optical detection (1). Fluorescence can attain detection limits of about  $10^8$  molecules/cm<sup>3</sup> for highly fluorescent large molecules. This limit is imposed by factors that include interference by indirectly scattered excitation light, losses imposed by filtration requirements, light collection losses, photomultiplier quantum efficiency loss, and kinetic bottlenecks to efficient optical pumping (i.e., triplet state buildup). For many molecules of interest, fluorescence quantum yields are small and fluorescence detection is impractical. Poor spectral selectivity is a severe limitation when analysis involves complex mixtures or firm identification is required.

Resonance enhanced two-photon ionization spectroscopy overcomes these limitations. It is applicable to weakly fluorescent molecules because ionization can be induced rapidly with respect to competing relaxation processes. Other features include: (1) near unit detection quantum efficiency can be achieved by using saturated excitation intensity combined with unit efficiency ion detection, (2) scattered laser radiation does not necessarily generate a background signal, (3) spectral selectivity can be achieved because R2PI requires that excitation can induce a one-photon electronic transition and that two photons have sufficient energy to reach the

ionization threshold, and (4) time-of-flight ion mass discrimination may be used to increase detection selectivity.

Recently, several research groups have begun studying multiphoton ionization of molecules in low pressure environments (2-9). Most of this work is based on interactions involving three or more photons with one nonresonant step. In particular, the studies by Johnson et al. (4) of molecules such as NO and benzene demonstrate that the ionization method provides high quality spectroscopic information and is a useful addition to the already developed fluorescence detection method of high resolution multiphoton spectroscopy (10, 11).

The approach pursued in the work described in this paper follows along lines of atomic resonance ionization spectroscopy (12). Whereas the spectroscopy and relaxation processes of atomic systems are moderately well understood, the corresponding molecular processes are far more complex and should be thoroughly investigated before practical detection procedures are established. In this paper, attention is given to aspects of the excitation process that influence naphthalene detection.

## EXPERIMENTAL

Naphthalene was chosen for investigation as a prototype polynuclear aromatic hydrocarbon for which extensive spectroscopic information is available. Commercial zone refined naphthalene was used in these studies. The experimental apparatus is depicted in Figure 2. Excitation was provided by a frequency-doubled flashlamp-pumped dye laser (Chromatix CMX-4). The ultraviolet output was isolated from the fundamental by an optical filter (F) and a portion of the ultraviolet output was deflected by a beam splitter (BS) to a photodiode (PD) intensity monitor (RCA 935) and the remainder of the output was focused along the axis of a cylindrical proportional counter cell using a 5-cm focal length lens (L). The wavelength was monitored by a spectrometer (SPEC). The proportional counter was constructed by suspending a tungsten wire anode of  $3 \times 10^{-3}$  cm diameter along the axis of the surrounding cylindrical cathode (inside diameter of 2 cm, length of 5 cm). The tubular copper cathode was supported inside an inclosed sample chamber by an insulating Teflon block and the cathode was operated at approximately -2100 V with respect to the grounded sample cell. The anode wire was connected directly to the input of a current amplifier (PAR 181) that supplied signal for a boxcar integrator (PAR 162). The triggering signal for the boxcar was supplied by an amplitude discriminator (Ortec 410) which was set to select excitation pulses with energy falling within  $\pm 5\%$  of a preselected window. This improved the long term reproducibility of measurement and provided approximate correction for wavelength dependence of the excitation pulse intensity. Laser intensity was adjusted during spectral scans to maximize the triggering rate.

Commercial P-10 counter gas (Matheson) consisting of 90% argon and 10% methane was used in the proportional counter in most experiments. A large thermostated chamber enclosed the vapor generator and sample chamber. The P-10 gas was passed through a thermal equilibration coil of copper tubing (EQ) and then through a vapor generator coil (VG) that had naphthalene coated on the inside walls. The P-10 gas containing saturated naphthalene vapor flowed through the proportional counter cell continuously at a flow rate of  $10 \text{ cm}^3/\text{s}$ . (Saturation was confirmed by monitoring the buildup of signal to constant intensity each time the temperature was incremented.) Optical

<sup>1</sup> Present address: Rocketdyne Division, Rockwell International, 6633 Canoga Avenue, Canoga Park, Calif. 91304.

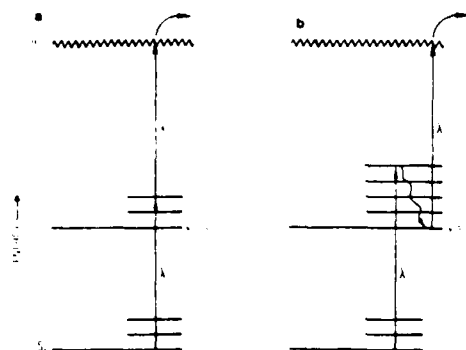


Figure 1. Schematic representation of energy levels of naphthalene. Case a depicts direct resonance enhanced two-photon ionization. Case b depicts the vibrational relaxation process in the intermediate electronic state  $S_1$ .

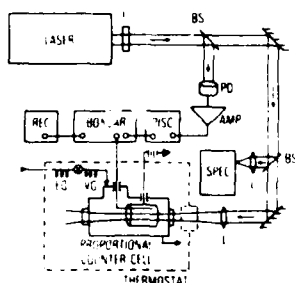


Figure 2. Block diagram of photoionization detection apparatus

access to the detection cell was provided by double windows fitted into the insulated walls of the thermostat chamber. Subambient temperatures were maintained by a feedback controlled supply of cooled nitrogen gas. An electric fan circulated nitrogen within the thermostat to achieve uniform temperature.

Proportional counter characteristics were studied prior to spectral investigations. Signals were generated with a CW mercury lamp which was capable of causing photoelectron ejection from the cathode surface. At low incident flux, the counter output consisted of isolated pulses of approximately  $10^{-6}$  s duration with amplitudes of about  $10^{-14}$  C. At higher UV flux, pulses overlapped and an average signal level could be measured. The logarithm of the signal level was found to be approximately linearly related to the applied voltage, as expected from a theoretical model of the proportional counter (13). The counter was also tested with pulsed UV laser excitation. No signal was observed with pure P-10 gas for excitation in the regions investigated, from 280–650 nm. When naphthalene was introduced at room temperature, signal levels of ca.  $10^{-6}$  C/pulse were obtained for excitation at 278 nm with a unit gain detector. This device was constructed from a pair of flat, parallel copper electrodes,  $1 \text{ cm}^2$ , with a separation of 0.5 cm between plates. One electrode was maintained at +200 V and the other electrode was connected to a preamplifier and boxcar integrator. At lower concentrations, signals were monitored using a proportional counter at gains in the range  $10^2$  to  $10^5$ . At low concentration and low intensity, the proportional counter signal was found to be a quadratic function of excitation intensity, as shown in Figure 3. At higher intensities the slope of the log-log plot of ion signal vs. excitation intensity approached unity, and at the highest intensities it was less than unity, indicating onset of saturation of ionization.

Experiments were repeated in the high intensity regime using the unit gain parallel plate ion current monitor which is not expected to display a significant space charge saturation effect. In the high intensity region, the slope for the parallel plate device was observed to be larger than that for the proportional counter. Therefore the high intensity data points in Figure 3 were measured with the parallel plate device and the slope at highest intensity (excitation pulse energy greater than  $10^3$  in Figure 3) was observed to be less than unity. This demonstrates that excitation intensity was sufficient to saturate the molecular photoionization process.

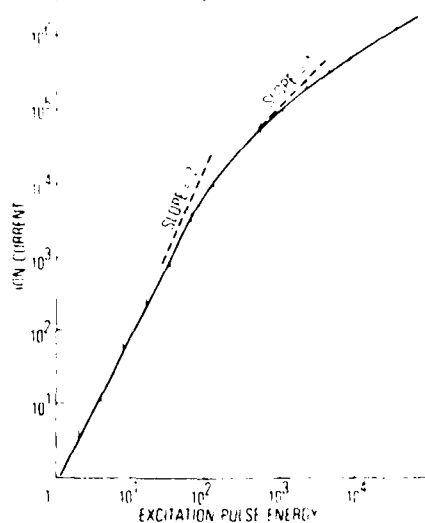


Figure 3. Saturation curve representing data points for ion current as a function of excitation pulse energy. Both scales are arbitrary and measurements go up to approximately 0.5 mJ/pulse UV excitation at 279 nm

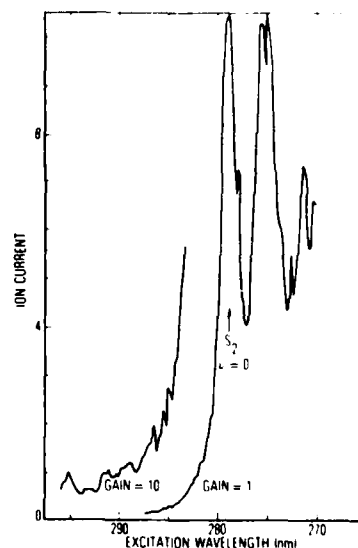


Figure 4. The naphthalene photoionization spectrum in the region of resonance with the second excited state  $S_2$

All spectral measurements performed with the proportional counter detection were obtained in the quadratic region.

To assess performance of the proportional counter in different environments, signal levels were measured for naphthalene in P-10, argon, nitrogen, and laboratory air. The signals obtained at -2100 V were 1, 1,  $10^{-3}$ , and  $10^{-5}$  in accordance with expectations based on electron affinities of these gases.

## RESULTS AND DISCUSSION

**Naphthalene Spectrum.** Figure 4 presents the most intense region of the naphthalene photoionization spectrum measured in P-10 gas at room temperature. Ion current was not observed for excitation wavelengths longer than 320 nm. The ground state ionization potential  $IP(0)$  of 8.14 eV (14) for naphthalene implies a theoretical threshold wavelength of 304 nm. Ion current increased rapidly with decreasing wavelength below 304 nm.

The strong signals obtained at 279 and 275 nm correspond to one-photon resonance with the second excited singlet state ( $S_2$ ) zero-point level and to the vibronic level  $S_2 + a_{1g}$  (9). In

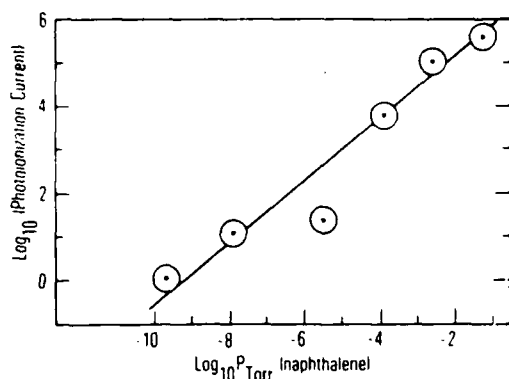


Figure 5. Logarithm of the proportional counter output current in arbitrary units (points) compared to the thermodynamically extrapolated vapor pressure corresponding to various experimental temperatures

this region the spectrum strongly resembles the one-photon spectrum. The 279- and 275-nm peaks are expected to provide the maximum sensitivity for ambient pressure detection. The intensity ratio of the 279-nm and 275-nm bands is the same within experimental uncertainty as the ratio observed in one-photon absorption. Based on the observed spectra, it can be anticipated that spectral selectivity is similar to that provided by one-photon ultraviolet spectroscopy. The requirement that two-photons equal or exceed the ionization potential ensures that species with higher ionization potentials such as benzene derivatives, alkenes, and alkanes will not cause spectral interference, even when they are present at concentrations orders of magnitude higher than naphthalene. Studies of spectral discrimination and mass discrimination between naphthalene derivatives will be reported at a later time.

**Detection Limits.** An experiment was performed to assess potential detection limits for the method. Naphthalene vapor concentration was controlled by varying the temperature of the naphthalene vapor generator tube and the proportional counter cell. The cell was cooled as a precaution to ensure that no excess naphthalene could be introduced by outgassing from porous Teflon and from trapped areas within the cell. It must be realized that the proportional counter response will vary slightly with temperature as a result of factors such as change in number density of the P-10 buffer gas (13). In Figure 5 the logarithm of the observed ion signal is plotted as a function of naphthalene vapor pressure. Excitation was provided at 279 nm using fluorol dye. Thermal equilibration times of 1 h were used as the temperature was lowered from 298 to 185 K. A weak spectral peak corresponding to the 279-nm band could be discerned with signal-to-noise ca. 2 at the 185 K level. The naphthalene pressure can be estimated by fitting available pressure data (15) in the range from 0.1 to  $5 \times 10^{-4}$  Torr by the expression:

$$\log_{10} P = \frac{-4570}{T} + 14.39 \pm \left[ \frac{98.3}{T} - 0.29 \right] \quad (1)$$

where  $P$  is pressure (Torr) and  $T$  is temperature (K). On this basis it can be estimated that the equilibrium naphthalene vapor density at 185 K is about  $3(\pm 2) \times 10^6$  molecules/cm<sup>3</sup> (ca.  $5 \times 10^{-11}$  Torr). This is five orders of magnitude below the value at room temperature and represents detection of less than 1 part in  $10^{12}$  parts buffer gas. The calculated vapor pressure scale is incorporated into Figure 5. This detection limit can be compared to fluorescence detection limits of about  $10^8$  molecules/cm<sup>3</sup> (calculated from data presented in Ref. 1, Table IV, p 74) which have been obtained for aromatic molecules in solution using laser excitation.

It is interesting to compare the estimated photoionization detection limit with the theoretical estimate for detection

sensitivity. Figure 3 indicates that the ion signal is near saturation. Therefore in theory it should be possible to approach detection of a single molecule in the interaction region. The laser interaction volume was measured and can also be estimated theoretically. Approximately 90% of the intensity passed through a  $10^{-3}$  cm<sup>2</sup> aperture at the focal point. The beam diameter doubles at  $\pm 0.5$  cm from the focal point. Therefore the maximum empirical volume for effective two-photon excitation was  $10^{-3}$  cm<sup>3</sup>. Using the calculated density of  $3 \times 10^6$  molecules/cm<sup>3</sup>, this implies that at the detection limit there were  $10^4$  or less molecules in the detection volume. This estimate is substantially larger than the theoretical estimate of one molecule. This discrepancy may be attributed to poor laser beam quality. One half the two-photon signal should be generated within the volume defined by the TEM<sub>00</sub> confocal parameter (interaction length of  $(8/\pi)^{1/2}\lambda$ ) and the diffraction limited beam diameter  $((4/\pi)^{1/2}\lambda)$ . This volume is calculated to be  $10^{-6}$  cm<sup>3</sup>. The flashlamp pumped dye laser source generates higher order modes which are not effective in exciting multiphoton processes because they are not focused as tightly as TEM<sub>00</sub>. A detection limit of 3 molecules calculated on the basis of the TEM<sub>00</sub> interaction volume provides a better correspondence to the theoretical ion detection sensitivity.

## CONCLUSIONS

Two-photon induced photoionization provides spectrally selective detection of naphthalene in an ambient pressure buffer gas. The spectrum is generally consistent with expectations based on the one-photon absorption spectrum, anticipated collision induced vibrational relaxation processes, and expected excited state photoionization characteristics. Extension to detection of other aromatic molecules of environmental concern appears to be promising. The technique can be implemented with simple components and can be interfaced with conventional chemical analysis instrumentation such as the gas chromatograph. Newly introduced high power dye lasers pumped by unstable resonator Nd:YAG lasers promise to increase the TEM<sub>00</sub> detection volume by many orders of magnitude. This should result in corresponding improvements in the ultimate detection limit.

Work is now in progress to establish the kinetics of the detection process, to investigate application to other molecular species, to establish the ultimate limit on selectivity, and to apply the method to detection of gas chromatograph effluents.

**Note Added in Proof.** Recently another group has applied R2PI to detection of aniline (16).

## ACKNOWLEDGMENT

We gratefully acknowledge R. Moler for valuable discussions concerning proportional counters.

## LITERATURE CITED

- (1) Winefordner, J. D. "Laser-Excited Luminescence Spectrometry" in "New Applications of Lasers to Chemistry", Hettler, G., Ed., Am. Chem. Soc. Symp. Ser. 1978, No. 85.
- (2) Held, B.; Mainfray, G.; Manus, C.; Morellec, J.; Sanchez, F., *Phys. Rev. Lett.* 1972, 28, 130-131.
- (3) Lineberger, W. C.; Patterson, T. A. *Chem. Phys. Lett.* 1972, 13, 40-44.
- (4) Johnson, P. M.; Berman, M. R.; Zakheim, D. J. *Chem. Phys.* 1975, 62, 2500-2502; Johnson, P. M., *ibid.* 1975, 62, 4562-4563; 1976, 64, 4638-4644.
- (5) Petty, Gena; Tai, C.; Dalby, F. W. *Phys. Rev. Lett.* 1976, 34, 1207-1209.
- (6) Parker, D. H.; Sheng, S. J.; El Sayed, M. A., *J. Chem. Phys.* 1976, 65, 5534-5535; Parker, D. H.; Berg, J. O.; El Sayed, M. A. *Chem. Phys. Lett.* 1978, 56, 197-199; Berg, J. O.; Parker, D. H.; El Sayed, M. A. *Chem. Phys. Lett.* 1978, 56, 411-413.
- (7) Feldman, D. L.; Leng, R. K.; Zare, R. N. *Chem. Phys. Lett.* 1977, 52, 413-417.
- (8) Herrmann, A.; Leutwyler, S.; Schumacher, E.; Wöste, L. *Chem. Phys. Lett.* 1977, 52, 418-425.

- (9) Zandee, L.; Bernstein, R. B.; Lichtin, D. A. *J. Chem. Phys.* 1978, 69, 3427-3429; Zandee, L.; Bernstein, R. B. *J. Chem. Phys.* 1979, 70, 2574-2575.
- (10) Bergman, A.; Jortner, J. *Chem. Phys. Lett.* 1972, 15, 309-315.
- (11) Bray, R. G.; Hochstrasser, R. M.; Wessel, J. E. *Chem. Phys. Lett.* 2, 1974, 27, 167-171; Hochstrasser, R. M.; Sung, H. M.; Wessel, J. E., *J. Am. Chem. Soc.* 1973, 95, 8179.
- (12) Hurst, G. S.; Nayfeh, M. H.; Young, J. P. *Appl. Phys. Lett.* 1977, 30, 229-231.
- (13) Williams, A.; Sara, R. I. *Int. J. Appl. Radiat. Isot.* 1982, 13, 229-238.
- (14) Rosenstock, H. M.; Draxl, K.; Steiner, B. W.; Herron, J. T. *J. Phys. Chem. Ref. Data*, 1977, Suppl. No. 1 to V. 1.6.
- (15) Hughes, E. E.; Liss, S. G. "Vapor Pressures of Organic Compounds in the Range Below One Millimeter of Mercury", *Natl. Bur. Stand. (U.S.) Tech. Note* 1960, No. 70.
- (16) Brophy, J. H.; Rettner, C. T. *Opt. Lett.* 1979, 4, 337-339.

RECEIVED for review August 28, 1979. Accepted November 12, 1979. This work was supported in part by the U.S. Air Force Office of Scientific Research under Grant AFOSR-77-3438, in part by the National Science Foundation under Grant CHE 77-16074, and in part by The Aerospace Corporation.



APPENDIX B

Ultrasensitive Detection of Aromatic Hydrocarbons by  
Two-Photon Photoionization

## Ultrasensitive detection of aromatic hydrocarbons by two-photon photoionization

Charles Klimcak and John Wessel

*Ivan A. Gettings Laboratories, The Aerospace Corporation, Los Angeles, California 90009*

(Received 17 March 1980; accepted for publication 5 May 1980)

An optimized multiphoton photoionization detection system has been applied to monitor aromatic-hydrocarbon vapor density as a function of temperature. The density curves established for naphthalene by this procedure permit estimation of a detection limit of  $5 \times 10^4$  molecules/cm<sup>3</sup> in a nitrogen buffer gas. With slight modification this method would be capable of single-molecule detection limits.

PACS numbers: 33.80.Kn, 06.70.Dn, 82.80.Di, 64.70.Hz

Recently several research groups have achieved detection limits in the single-atom regime using photoionization-

and fluorescence-based techniques.<sup>1-5</sup> Attainment of molecular detection at densities approaching this limit is of consid-

erable importance for various research applications and eventually will be important for monitoring and surveillance applications. Aromatic hydrocarbons in particular represent a large class of environmentally important carcinogens and potential carcinogens for which improved detection capability is sought. Typical detection limits achieved for large polyatomic species using the most sensitive spectroscopic methods such as laser-excited fluorescence and gas-chromatography/mass-spectrometry have been on the order of  $10^8$  molecules/cm<sup>3</sup>.<sup>6</sup> The best detection limits reported for small molecules such as OH and for diatomic species in closed detection cells are on the order  $10^6$  molecules/cm<sup>3</sup>.

In this letter we describe development of an ultrasensitive molecular vapor detection system based on resonance-enhanced two-photon photoionization spectroscopy (R2PI).<sup>8,9</sup> The R2PI method provides the potential to approach single-molecule detection limits for a broad range of species based on ability to detect creation of a single ion-electron pair. The new results demonstrate three-orders-of-magnitude improvement with respect to prior detection capability. Naphthalene has been selected for study because it has properties representative of the important class of large aromatic molecules that can be detected with equivalent sensitivity<sup>10</sup> by R2PI. New advances have been obtained by developing an improved ionization cell in combination with an advanced tunable laser which overcomes the problem of a source intensity-limited signal. Procedures have been implemented to ensure that the photoionization signal can be linearly related to the naphthalene number density.

The experimental configuration which was described in detail previously is shown in Fig. 1. For the new work an ionization cell was constructed of clean stainless-steel-with-Varian-type flanges and sapphire windows. The windows were positioned on 0.5-m extension arms extending away from the ion detection region and baffles were inserted in the extension arms to prevent electrons, ions, and scattered light generated at the windows from reaching the detection region. High-purity naphthalene was extensively zone refined.

Experiments were carried out using pure nitrogen and pure argon buffer gases. Impurity contamination was mini-

mized by using liquid-nitrogen boil-off and by passing research-grade argon through a coil of tubing cooled to 140 K, well below the lowest vapor generator temperature. The ionization cell and associated apparatus were vacuum baked at 473 K prior to introduction of carrier gas. In one set of experiments the naphthalene vapor density was controlled by varying the temperature of the thermostat containing the vapor generator coil and the photoionization cell. In a second set of experiments the photoionization cell remained at room temperature and the vapor generator coil was cooled to establish the desired vapor pressure. Approach to equilibrium between vapor and solid phases was followed by monitoring signals as a function of time and flow rate subsequent to temperature adjustment.

Excitation intensity was adjusted to maintain ionization signals within the linear range of the detectors at all vapor densities. A quadratic dependence on excitation intensity prevailed at the vapor densities studied, provided the ionization current was within the linear response range of the detectors. This dependence was used to scale the photoionization signal levels. For unit-gain experiments temperature-independent response was achieved by applying a collection voltage (100 V) within the plateau region (10–500 V) of unit-gain charge collection. A charge-sensitive preamplifier (Amptek A203) was attached directly to the cell for these experiments. Measurements requiring the greatest amplification were made using an argon carrier gas with proportional counter gain of 20.

Excitation by the frequency-doubled output of a Nd:YAG pumped dye laser was adjusted to obtain a maximum of 1 mJ/pulse at 278.5 nm. A beam diameter of approximately 1 mm, a pulse duration of approximately 5 ns, and a linewidth of  $5 \times 10^{-3}$  nm were used. Naphthalene has an absorption maximum corresponding to  $S_2 \leftarrow S_0$  at 278.5 nm and a minimum at 277.5 nm. The naphthalene signal was taken to be proportional to the difference between response at these two wavelengths. In some experiments background signals were observed, presumably due to inadvertent contamination. In all cases the background signals were substantially higher at 277.5 than 278.5 nm. Therefore naphthalene signals can be identified with confidence. Under the cleanest experimental conditions, no background was observed above amplifier noise at the lowest temperatures for which a good signal was obtained (160 K).

Broadening of the  $S_2 \leftarrow S_0$  transition due to spectral congestion greatly exceeds thermal broadening and the rate of ionization from the intermediate state exceeds the temperature-dependent natural decay rate of the intermediate state. Therefore temperature dependence of the two-photon ionization cross section can be neglected.

The log of the observed photoionization signals are plotted on the left-hand vertical axis of Fig. 2 as a function of  $T^{-1}$ . The data points span eight orders of magnitude, maintaining approximate linearity. Measurements made with the cooled-cell procedure are believed to be more reliable than those made at constant temperature because thermal equilibrium between solid and vapor phase naphthalene was assured in the former case. Higher-pressure measurements were performed with a capacitance manometer. These re-

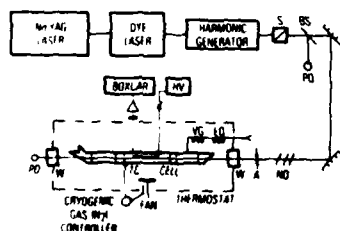


FIG. 1. Block diagram of experimental apparatus. Glan prism *S* separates the second-harmonic excitation beam from the dye-laser fundamental, the beam splitter *BS* deflects a portion of the beam to a reference photodiode *PD*, the beam is attenuated appropriately by neutral density *ND*, the beam diameter is adjusted by aperture *A*, the beam passes through insulating window *W*, carrier gas is passed through thermal equilibration coil *EQ*, naphthalene is introduced into the carrier gas from solid surfaces coated with naphthalene crystals in vapor generator *VG*, and the cell temperature is sensed and controlled by the thermocouple *TC*, which is rigidly attached to the cell body.

sults are plotted on an expanded scale in the insert to Fig. 2 and are repeated on the compressed vertical scale appearing on the right-hand side of Fig. 2. The slopes recorded in Fig. 2 differ significantly from values deduced from earlier recommended data<sup>11</sup>; however, measurements recommended more recently<sup>12,13</sup> are in close agreement over the range 253–298 K. Additional independent measurements were performed in the range 200–273 K using fluorescence detection in order to confirm the slope at lower temperatures. These experiments were carried out with a sealed cell which was cooled to the measurement temperature. The slope was the same within experimental error as the slope measured by photoionization.

The following procedure was used to relate the ionization current signals to the naphthalene number-density scale. Capacitance manometer pressure data were fit by linear least squares and evaluated at 273 K. The photoionization data were least-squares fit to another linear equation and the constant term was readjusted by addition of scaling constant  $\Delta$ , so that the calculated value of  $\log_{10} n$  matched that calculated at 273 K from the equation for the capacitance manometer. Then  $\Delta$  was added to the photoionization data points and they were plotted using the right-hand vertical scale of Fig. 2.

The signals recorded at 166 K with a number density of  $\sim 7 \times 10^5 \text{ cm}^{-3}$  and at 160 K ( $\sim 1 \times 10^5 \text{ cm}^{-3}$ ) are shown in Fig. 3. At 160 K the signal level corresponds to approximately  $10^3$  electrons/pulse. This is near the noise limit of the amplifier and it corresponds closely to the signal expected at  $10^5 \text{ molecules cm}^{-3}$  on the basis of the  $\sim 0.1\text{-cm}^3$  interaction volume combined with excitation near optical saturation intensity.

The theoretical vapor density curve shown in Fig. 2 has been calculated using recent calorimetric data.<sup>12,13</sup> The Clausius-Clapeyron equation was integrated from 273 K to temperatures of interest using the approximation

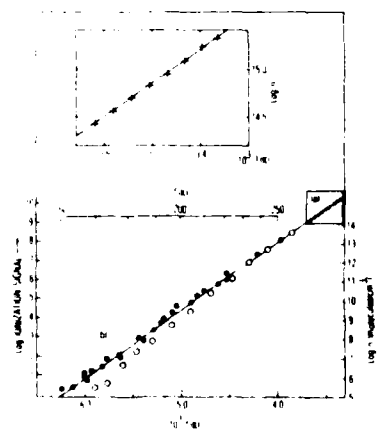


FIG. 2. Naphthalene vapor number-density measurements: (a) Number densities deduced from capacitance manometer pressure measurements. (b) Ionization signals and number densities derived from the low-temperature ionization cell measurements are displayed as solid dots and for room-temperature ionization cell measurements by open circles. The solid line represents the theoretical vapor pressure calculated from calorimetric data.

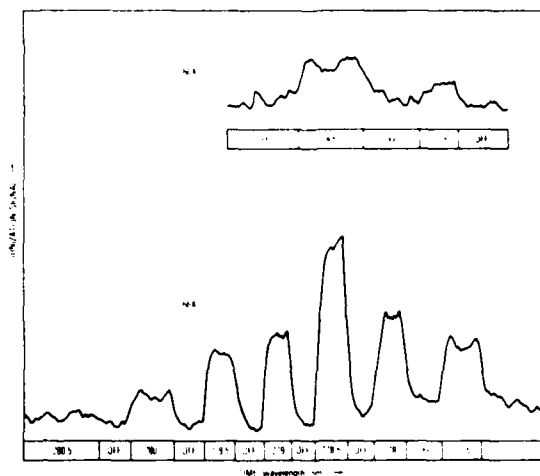


FIG. 3. Representative signals of naphthalene in argon carrier gas observed near the detection limit. Excitation is successively stepped to wavelengths spanning the origin of the naphthalene  $S_2 \leftarrow S_0$  transition in the 167-K measurement. The source is temporarily off between each measurement wavelength. At 160 K, where the density is  $10^5 \text{ cm}^{-3}$ , signal to noise is approximately 4.

$\Delta H_{\text{vap}}(T) = 70\,660.6 - 20.21(T - 200) \text{ J/mol K}$ , where the constants for the gas phase are recently recommended values<sup>13</sup> and the solid phase enthalpy has been taken from a prior reference.<sup>14</sup> The correspondence between experimental points and the thermodynamic curve is excellent considering the substantial possibility for systematic error. The detection limit of  $5 \times 10^4 \text{ cm}^{-3}$  ( $S/N \sim 2$ ) derived from this work represents an improvement of  $\sim 10^3$  with respect to the previously reported 185-K photoionization detection limit. Additional improvement by a factor ranging from 10 to 100 could be sought given improved performance of the proportional counter-amplifier system. A factor of 100 improvement would correspond to detection of 50 molecules in the laser interaction region. This is approximately the number of molecules required to ensure that one molecule is present in an initial quantum state that can interact with the laser source. Single-molecule detection could be obtained by tailoring the excitation source to interact with the entire ground-state population. An increase in spectral bandwidth or an increase in laser pulse duration would be effective.

The authors would like to express appreciation to Dr. Jerry Gelbwachs for stimulating discussions concerning this work and for helpful comments regarding preparation of the manuscript. This work was supported by the Air Force Office of Scientific Research under Grant AFOSR-77-3438, by the National Science Foundation under Grant CHE-77-16074, and by the Department of Energy, Office of the Environment under Contract 79EV10239.000.

<sup>1</sup>W. M. Fairbank, Jr., T. W. Hansch, and A. L. Schawlow, *J. Opt. Soc. Am.* **68**, 199 (1975).

<sup>2</sup>G. S. Hurst, M. H. Nayfeh, and J. P. Young, *Appl. Phys. Lett.* **30**, 229 (1977).

<sup>3</sup>G. W. Greenless, D. L. Clark, S. L. Kaufman, D. A. Lewis, J. F. Tonn, and J. H. Broadhurst, *Opt. Commun.* **23**, 236 (1977).

<sup>4</sup>V. L. Balykin, V. S. Letokhov, V. I. Mishin, and V. A. Semchishen, *JETP Lett.* **26**, 357 (1977).

<sup>5</sup>J. A. Gelbwachs, C. F. Klein, and J. E. Wessel, *IEEE J. Quantum Electron.* **QE-14**, 121 (1978).

<sup>6</sup>J. D. Winefordner, *ACS Symp. Ser. 85*, edited by G. Hieftje (American Chemical Society, Washington, D.C., 1978), pp 50-79.

<sup>7</sup>C. C. Wang and L. I. Davis, Jr., *Phys. Rev. Lett.* **32** 349 (1974).

<sup>8</sup>R. P. Frueholz, J. E. Wessel, and E. Wheatley, *Anal. Chem.* (in press).

<sup>9</sup>J. H. Brophy and C. T. Rettner, *Opt. Lett.* **4**, 337 (1979).

<sup>10</sup>C. M. Klimcak and J. E. Wessel, *Anal. Chem.* (in press).

<sup>11</sup>E. E. Hughes and S. G. Kias, *Natl. Bur. Stand. Tech. Note 70* (U.S. Dept. Commerce, Washington, D.C., 1960).

<sup>12</sup>E. J. Morawetz, *J. Chem. Thermodyn.* **4**, 455 (1972).

<sup>13</sup>S. S. Chem, S. A. Kudchadker, and R. C. Wilhoit, *J. Phys. Chem. Ref. Data*, **527** (1979).

<sup>14</sup>J. P. McCullough, H. L. Finke, J. F. Messerly, S. S. Todd, T. C. Kincheloe, and G. Waddington, *J. Phys. Chem.* **61**, 1105 (1957).

## APPENDIX C

### Gas Chromatography with Detection by Laser Excited Resonance Enhanced 2-Photon Photoionization

## Gas Chromatography with Detection by Laser Excited Resonance Enhanced 2-Photon Photoionization

Charles M. Klimcak and John E. Wessel\*

*Ivan A. Getting Laboratories, The Aerospace Corporation, P.O. Box 92957, Los Angeles, California 90009*

Resonance enhanced 2-photon photoionization has been applied to detection of gas chromatograph effluents using a small volume proportional counter cell and a low power laser. Detection limits on the order of 10 picograms were obtained for the aromatic hydrocarbons anthracene, phenanthrene, benzanthracene, acenaphthene, naphthalene, and assorted halonaphthalenes. Spectral differentiation between coeluting anthracene and phenanthrene was also demonstrated. The influence of excitation pulse duration was investigated.

There is an increasing need for selective gas chromatographic detectors with high sensitivity. In this report, we describe application of resonance enhanced 2-photon photoionization (R2PI) to detection of chromatographic effluents. Spectrally selective detection of several aromatic hydrocarbons is demonstrated. At ambient pressure the process, which is shown in Figure 1, involves excitation from ground state  $S_0$  to excited state  $S_2$ , followed by collisionally induced relaxation to  $S_1$  and subsequent ionization. This new method which has been described in recent reports (1-3) is applicable to most

molecular species, and is expected to attain sub-picogram detection limits. Related multiphoton photoionization methods have been applied extensively for molecular spectroscopic investigations (4-25) and R2PI has been used for single atom detection (26, 27).

Recently a commercial photoionization detector based on one-photon photoionization induced by an incoherent UV source has achieved widespread use for gas chromatographic applications (28, 29). This device, whose development was based on extensive prior photoionization work, provides limited although highly valuable spectral selectivity in that the photon energy can be chosen in order to selectively ionize species with low ionization potentials while leaving species with higher ionization potentials unexcited (28). Thus, aromatics can be detected in the presence of higher concentrations of alkanes. By utilizing short wavelength UV sources, all molecules of interest can be ionized; therefore the method is widely applicable. Picogram detection limits have been obtained in favorable cases.

The multiphoton detection method studied in this report offers the following potential advantages with respect to conventional one-photon photoionization detection: (1) greatly

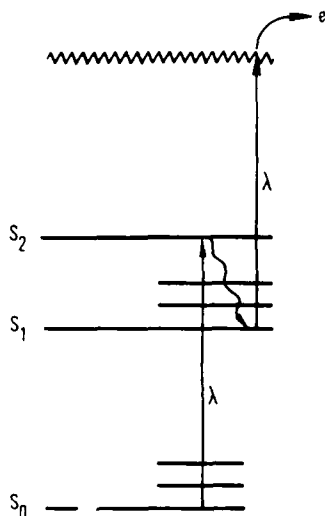


Figure 1. Ambient pressure two-photon photoionization process

increased spectral selectivity, (2) improved ionization efficiency, (3) decreased detection volume in applications involving capillary columns, and (4) ion mobility may be measured to provide additional selectivity. A tunable laser source is used for the R2PI method. In the predominate excitation process occurring at ambient pressure shown in Figure 1, a first photon promotes a strong 1-photon transition in the species of interest, corresponding to the transition observed in conventional UV absorption spectrometry. The molecule then undergoes vibrational relaxation in the excited electronic state. The second photon ionizes the vibrationally relaxed excited state molecule. Therefore the R2PI excitation spectrum resembles the UV absorption spectrum; however, the second photon must have sufficient energy to ionize the excited state. As a result there is a fairly sharp onset wavelength for ionization. Species with higher ionization potentials are not ionized; therefore the method can provide excellent background rejection. By using high excitation intensity (approaching optical saturation of the ionization process), nearly uniform detection efficiency can be achieved for different molecular species, including those with weakly fluorescent excited states.

The potential for ultrasensitive detection is based on the feasibility of ionizing nearly all interacting molecules contained in the detection cell. The ability to achieve the required condition of optical saturation was demonstrated in a previous report (1). Although the low power lasers used in this study did not approach the capability of saturating the detection cell volume, high power tunable lasers with this ability are commercially available. Ionization efficiency inside the saturated excitation volume is about three orders of magnitude higher than for one-photon ionization by incoherent UV ionization sources. Ionization events in the laser interaction volume are detected by a proportional counter, which can respond to a single ion-electron pair. By using a tightly collimated laser beam, the detector cell volume can be made comparable to capillary column dimensions. Therefore it is theoretically possible to approach single molecule detection limits in a small volume gas chromatograph detector cell.

The major objectives of this study have been to: (1) demonstrate detection by R2PI in a small volume proportional counter cell at the elevated temperature required for chromatography, (2) demonstrate that R2PI is applicable to aromatic species with differing excited state properties, and (3) show that appreciable spectral selectivity can be achieved. No attempt has been made to optimize detection limits or to

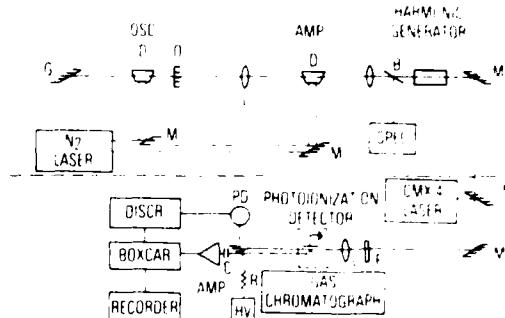


Figure 2. Photoionization detection apparatus

optimize chromatographic resolution (work was performed with a low power laser system and a low resolution isothermal chromatograph). The results demonstrate that a broad range of aromatic hydrocarbons can be detected using short wavelength excitation and selective detection can be obtained for some species using carefully chosen longer wavelengths.

## EXPERIMENTAL

**Laser.** Two different types of pulsed lasers shown in Figure 2 were used in order to assess effects of pulse duration on the ionization process. A Chromatix CMX-4 flashlamp pumped dye laser was equipped with intracavity frequency doublers and was tuned over the range from 335 to 270 nm. It provided pulses with a duration of 1  $\mu$ s and a maximum available energy per pulse of 200  $\mu$ J at 300 nm. Mirror  $M_1$  introduced this beam into the optical path and blocked the upper laser system. Shorter pulses having a duration of 5 ns were obtained with a transversely pumped dye laser of the configuration developed by Hansch (30). The oscillator was optically pumped by a portion of the output of a nitrogen laser (NRG-0.5-5-150/B). The diffraction grating (G) was a 60° blazed eschelle with 300 grooves per mm. Dye cuvettes (D) in the oscillator (OSC) and amplifier (AMP) were stirred by magnetic stirrers and were transversely excited by (geometrically divided) portions of the nitrogen laser beam. A beam splitter (B) deflected a portion of the dye laser beam to a spectrometer (SPEC) which measured the output wavelength and the remainder of the fundamental was frequency doubled into the UV by an angle tuned KDP harmonic generator crystal. At 300 nm, the maximum available energy per pulse was 10  $\mu$ J. Residual visible laser light was removed from the beam by a Corning 7-54 colored glass filter (F) and the ultraviolet light was focused into the ionization detector with a 100-mm focal length fused silica lens. This results in an effective multiphoton focal volume of  $2 \times 10^{-6}$  cm<sup>3</sup> ( $(64/\pi^2) \lambda^3$ ). Rhodamine 640, rhodamine B, rhodamine 6G, and coumarin 495 dyes (Exciton Corp.) were used to cover the spectral regions of interest.

**Ionization Detector Configuration.** An exploded view of the ionization cell is illustrated in Figure 3. The stainless steel body was constructed from a 1/4-inch Swagelok "Tee" connector that was drilled out and fitted with fused silica windows to accommodate the entrance and exit of the laser. They were fastened to the cell by metal plates contiguous with the windows and screwed together to exert pressure on Viton O-rings placed between the windows and the cell body.

An anode for the collection of photoelectrons was fashioned from a  $5 \times 10^{-3}$  cm diameter tungsten wire shaped into a 0.3-cm diameter loop and mechanically bound to the inner conductor of a high voltage BNC connector. The outer casing of the BNC had been removed and the Teflon insulation machined to fit snugly inside the Swagelok "Tee". The anode assembly was wrapped with additional Teflon tape before being inserted into the Tee fitting in order to ensure a tight seal and the absence of voids.

**Signal Acquisition.** The high voltage (HV) dc applied to the anode signal collection wire through a 30-M $\Omega$  resistor (R) was capacitatively blocked with a 500-pf capacitor (C) prior to signal amplification. This made it possible to maintain ground potential at the cell body, which served as the cathode. Output from a current sensitive amplifier (AMP, PAR model 181) was routed



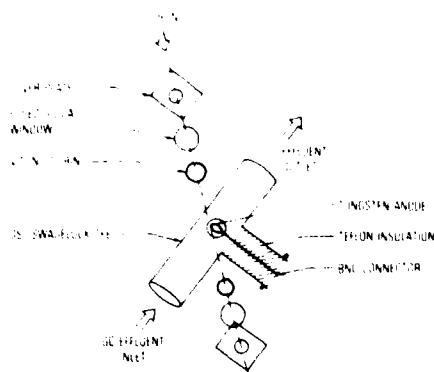


Figure 3. Ionization chamber

to a boxcar integrator (PAR model 162) equipped with a gated integrator (PAR model 164). The boxcar was adjusted for a 1- $\mu$ s duration gate which was commensurate with the proportional counter response time and was set for time coincidence between the gate and the excitation pulse. The time constant was chosen to provide 90% of full response after 5 trigger events.

Earlier studies of proportional counter characteristics had demonstrated that each photoevent resulted in a cascade of electrons of about 1- $\mu$ s duration. With the present anode geometry, an electron gain of approximately  $10^4$  was realized at an applied potential of 1250 V. Electron multiplication was found to be somewhat dependent on the focal position of the laser beam in the detector, thus precluding absolute measurement of the gain. In order to optimize detection sensitivity and selectivity, studies were undertaken to determine the excitation wavelength dependence of the multiphoton photoionization cross section. These experiments were performed with a vapor generator in which temperature was controlled to provide the desired partial pressure of the species. A standard proportional counting gas consisting of 90% argon and 10% methane (P-10, Matheson) was passed through the vapor generator into the ionization detector. In order to suppress noise caused by pulse-to-pulse variations of laser intensity and in order to compensate for changes in laser output as a function of wavelength, pulse-height energy discrimination was used. A discriminator (DISCR, Ortec 402) was set to trigger the boxcar detector (PAR 162) when the laser excitation pulse energy (measured by reference photodiode PD (RCA 935)) was within  $\pm 5\%$  of a preset level. Signals were rejected when excitation energy was outside this range. Laser pump intensity (flashlamp energy for CMX-4 or  $N_2$  laser pump energy for the Hansch type laser) was adjusted to maximize the triggering rate, (typically about 3 Hz when the laser was pulsed at 15 Hz). This procedure improved long term signal stability by a factor of  $\sim 4$ .

**Chromatograph Operating Conditions.** A 1.3 m  $\times$  3 mm stainless steel column packed with 80/100 mesh Chromosorb W coated with 3% OV-17 (Applied Science) was used in an isothermal gas chromatograph (Beckman GC-2A). P-10 gas at a flow rate of 20 mL/min served as both the carrier gas and the electron multiplication medium. The column and ionization detector were mounted in an oven that was operated at 468 K for the halogenated naphthalene studies and at 498 K for the aromatic hydrocarbon studies.

**Reagents.** Distilled in glass spectra grade acetone (Burdick and Jackson) was used as a solvent for this study. The naphthalene, anthracene, and phenanthrene had been extensively zone refined to eliminate unwanted impurities that might produce inaccurate photoionization spectra. The remaining materials were reagent grade (Eastman) and they were used without further purification. Prior to performing the photoionization experiments the presence of potentially interfering contaminants was investigated and the retention time of the major component was measured with the aid of a thermal conductivity detector in place of the ionization cell.

## RESULTS

**Spectral Selectivity.** The vapor generator studies of anthracene at 328 K and of phenanthrene at 358 K yielded

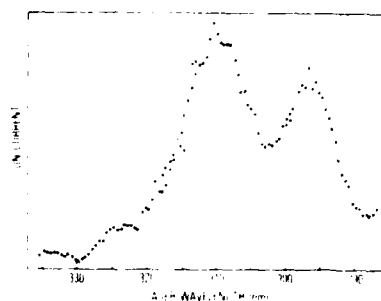


Figure 4. Two-photon ionization spectrum of anthracene obtained with the nitrogen pumped dye laser

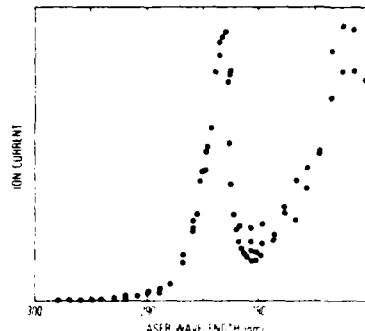


Figure 5. Two-photon ionization spectrum of phenanthrene obtained with the nitrogen pumped dye laser

the multiphoton ionization spectra shown in Figures 4 and 5. In each case, the ion current was observed to be quadratically dependent on the ultraviolet laser power at low intensity, indicating a two-photon ionization process. A thorough analysis of these spectra is currently in progress and the results will be published at a later date. For the present study, it is sufficient to note that variable detector selectivity can be obtained by the appropriate choice of laser wavelength. Detector response can be maximized for either isomer in a mixture of both with a high rejection ratio for the other component. Alternatively, an approximately equal response to each species is available when one employs an exciting wavelength in the region of spectral overlap.

A thermal conductivity detector was initially used to measure the retention characteristics of anthracene and phenanthrene in the packed column. These isomers could not be resolved; therefore separate 1- $\mu$ L injections of equimolar solutions (1  $\mu$ g/ $\mu$ L) were used. Anthracene and phenanthrene retention times were 3.87 and 3.65 min, respectively, with full widths at half-maximum of 0.35 min. Accurate quantitation of a mixture containing only a trace amount of one component was therefore deemed impossible using this column with a nonselective detector.

Analogous measurements with the multiphoton ionization detector confirmed our initial expectations of excellent selectivity and produced the striking chromatograms in Figure 6. These measurements were performed with the nitrogen pumped dye laser at a peak power of 1 kW. Consecutive injections of the two isomers were made at constant excitation energy and each chromatogram was measured with the same recorder sensitivity. The poorer signal-to-noise ratio at 285 nm was due to severe pump laser instability ( $>25\%$  pulse-to-pulse intensity fluctuations) that was occasionally encountered. Rejection ratios (defined as the relative detection advantage of anthracene with respect to phenanthrene measured at the chromatograph temperature of 498 K) were determined at 100 $\times$  sensitivity and were found to be 400 at 310 nm and 0.01 at 285 nm. The calculated rejection ratios could

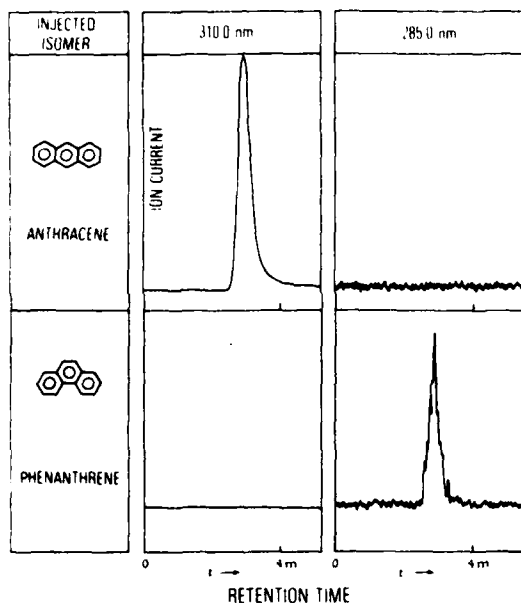


Figure 6. Illustration of the tunable selectivity of R2PI detection of a PAH isomer pair

conceivably be affected by the presence of photoionizable impurities in each pure species (including the isomer for which detection capability has been optimized) and hence represent lower limits of selectivity. The inadequate resolution of the present GC prevented a determination of isomeric contaminants in the neat materials. Nevertheless we have been able to quantitate mixtures of anthracene and phenanthrene in the mixing ratio regime of  $1:10^3$  under unfavorable chromatographic conditions by using multiphoton ionization detection.

#### Detector Sensitivity and Linear Dynamic Range.

Equal volumes of successively diluted anthracene stock solution ( $1 \mu\text{g}/\mu\text{L}$ ) were injected to determine the limit of detection and linearity of response. Nitrogen laser pumped dye laser excitation (kW peak power) was provided at 310 nm, the peak wavelength for anthracene detection. Elution profiles of the resulting ion current chromatograms did not vary with concentration; therefore the peak height was assumed to characterize the quantity of solute injected. After determining the detection limit, several blank runs of pure solvent were performed to ensure that solvent induced bleeding of solute retained by the column was not influencing this value. The minimum detectable amount of anthracene (with a S/N of 2) was extrapolated to be 10 pg. The ion current chromatogram resulting from a  $1/2 \mu\text{L}$  injection of a solution containing  $64 \text{ pg}/\mu\text{L}$  of anthracene is reproduced in Figure 7. The acetone solvent peak has been shown to result from an  $n$ -photon ionization process with  $n \geq 3$ . A constant background ionization signal was observed, independent of solvent injection. This background signal, which was quadratically dependent on excitation intensity, was probably due to multiphoton photoionization of materials that are being continually evaporated from the column. In the chromatogram of Figure 7, the peak response to the elution of anthracene is approximately one tenth of this residual background level.

Consecutive injections of higher concentration solutions were made to obtain the calibration curves of Figure 8. Detector saturation (presumably due to anodic space charge effects) was initially noticeable with the higher concentration solutions. Reduction of the anode potential (i.e., electron gain) was found to be a suitable means of extending linearity. Each

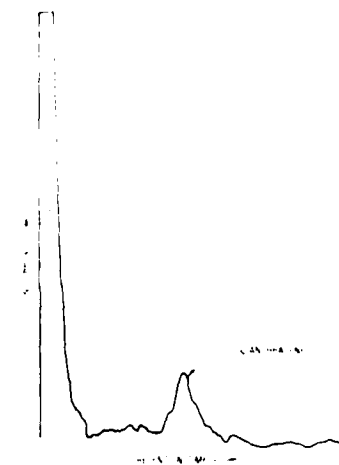


Figure 7. R2PI chromatogram obtained following the injection of  $1/2 \mu\text{L}$  of a  $64 \text{ pg}/\mu\text{L}$  solution of anthracene in acetone

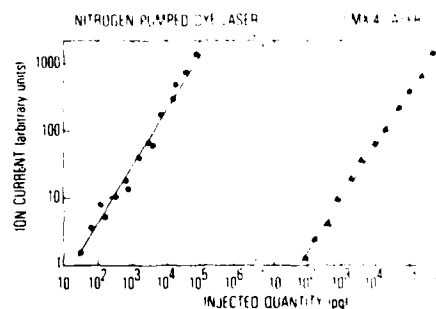


Figure 8. Calibration curves representing the R2PI detector response to anthracene plotted vs. the mass of anthracene injected for both laser excitation sources

curve of Figure 8 is actually a composite of curves taken at two operating voltages (750 and 1000 V) which have been normalized and joined (at 10 ng). The measured slopes of the plots of log signal vs. log concentration are 0.9 and 0.8 for nitrogen pumped and CMX-4 excitation, respectively. These differ substantially from a slope of unity for linear response, presumably as a result of ion current saturation effects.

**Applicability to PAH Detection.** An equimolar mixture of 5 polycyclic aromatic hydrocarbons (containing  $0.2 \mu\text{g}/\mu\text{L}$  of anthracene as an internal standard) was used to investigate the feasibility of multiphoton ionization detection of several polynuclear aromatic hydrocarbons (PAH) using a single excitation wavelength. The five components (naphthalene, acenaphthene, anthracene, pyrene, and 1,2-benzanthracene) were chosen for their relatively short retention times and ease of chromatographic separation under the isothermal operating conditions. Excitation at 303 nm was selected to guarantee that the two-photon energy exceeded the ionization potential for each species. Photoionization signals were observed for each component of the mixture using either the Chromatix or nitrogen dye laser. A typical ion current chromatogram is illustrated in Figure 9. From the relative integrated areas of each component and the observed anthracene detection limit we have calculated the minimum detectable quantities given in Table I based on 303-nm excitation.

Spectra were not obtained for pyrene, acenaphthene, and 1,2-benzanthracene, therefore optimum detection wavelengths and corresponding minimum detection limits are not yet known for these compounds.

**Applicability to Molecules with Varying Excited State Properties.** Detection methods such as fluorescence exci-

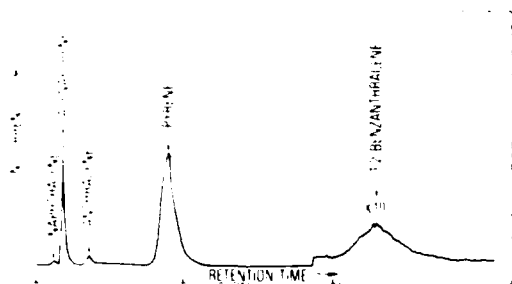


Figure 9. R2PI chromatogram of an equimolar mixture of polycyclic aromatic hydrocarbons obtained with the CMX-4 excitation source

Table I. PAH Detection Limits Pumped Dye Laser System Obtained Using the Nitrogen Laser

	detection limit, pg
anthracene	10
naphthalene	0.3
phenanthrene	50
acenaphthene	10
pyrene	6
1,2-benzanthracene	4

tation spectroscopy are highly dependent on the excited state radiative properties. In particular, the fluorescence quantum yields, which may range from unity to values as small as  $10^{-5}$  for derivatives of a particular PAH species, are a major factor in determining the ultimate detection limit. The two-photon photoionization method employs the same excited states used in fluorescence; therefore it is important to explore the influence of excited state properties on the R2PI process.

A series of halo-naphthalene derivatives was drawn for study. The excited state lifetimes and fluorescence quantum yields for the states of these molecules decrease rapidly as halogens of increasing atomic number are substituted. Values for these quantities compiled from several sources are shown in Table II. (It is virtually impossible to detect dibromonaphthalene and iodonaphthalene by fluorescence detection.) Nonetheless, the absorption spectra and ionization potentials are close to those for naphthalene. A solution containing an equimolar mixture of these halonaphthalenes in acetone was injected into the chromatograph system and laser excitation was provided at 305 nm, for which each of these compounds has a similar 1-photon absorption cross section corresponding to  $S_1 \leftarrow S_0$ . The relative integrated responses obtained with 5-ns duration excitation pulses for a solution containing equimolar quantities of naphthalene, 1-chloronaphthalene, 2-bromonaphthalene, 1-iodonaphthalene, and 1,4-dibromonaphthalene were 1, 0.7, 0.4, 0.5, 1, as shown in Figure 10a. For comparison the response obtained for excitation with 1- $\mu$ s excitation pulses is presented in Figure 10b. In this sample, the quantity of naphthalene was reduced by a factor of 100 whereas quantities of other components are equal in Figures 10a and 10b.

### DISCUSSION

The demonstration of spectral discrimination between anthracene and phenanthrene was possible because of the appreciable differences in their one-photon absorption spectra. For molecules with similar one-photon spectra and equivalent ionization potentials such as alkylated aromatic derivatives or halogenated derivatives, this opportunity may not exist. Time resolved ion mobility measurement might provide additional discrimination. It is possible that use of two separate wavelengths for the first and second photon can improve the spectral resolution capability substantially. The general

Table II. Fluorescence Lifetimes and Quantum Yields

	$\tau$		$\phi_f$	
	condensed phase	vapor phase	condensed phase <sup>a</sup>	vapor phase
naphthalene	100 ns <sup>b</sup>	170 ns <sup>c</sup>	0.3	0.18 <sup>d</sup>
1-chloronaphthalene	10 <sup>e</sup>	< 20 ns <sup>c</sup>	0.03	
1-bromonaphthalene	0.3 <sup>e</sup>		$8 \times 10^{-4}$	
1-iodonaphthalene	< 0.1 <sup>e</sup>	$\sim 0.9$ ps <sup>f</sup>	$< 2 \times 10^{-4}$	

<sup>a</sup> Ermolaev, V. L. *Sov. Phys. Usp.* 1963, 80, 333.

<sup>b</sup> Bonneau, R.; Faure, J.; Joussot-Dubien, J. *Chem. Phys. Lett.* 1968, 2, 65-67. <sup>c</sup> This work, measured with an ambient pressure N<sub>2</sub> buffer gas at 198 K. <sup>d</sup> Stockburger, M.; Gattermann, H.; Klusman, W. *J. Chem. Phys.* 1975, 63, 4529-4540. <sup>e</sup> Estimated from  $\tau = \phi_f/k_f$ . <sup>f</sup> Dzvonik, M.; Yang, S.; Bersohn, R. *J. Chem. Phys.* 1974, 61, 4408-4421.

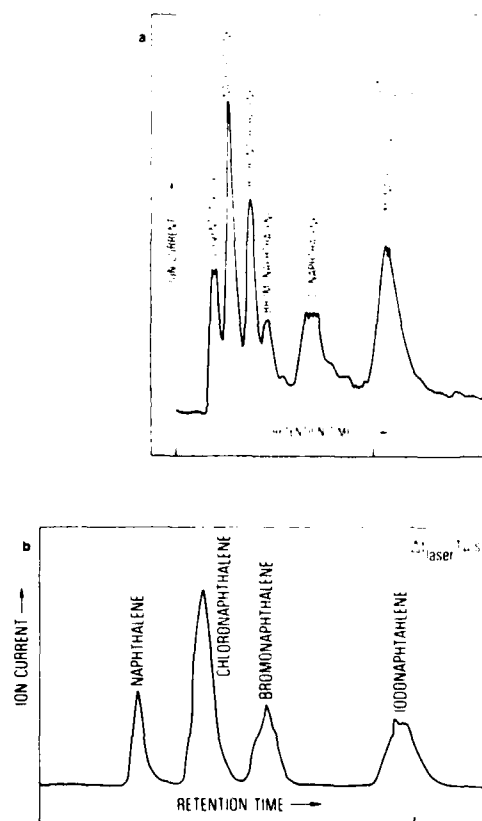


Figure 10. R2PI chromatogram of (a) equimolar mixture of halonaphthalenes using 5-ns excitation pulses and (b) a mixture of 2 ng of naphthalene with 200 ng of each halonaphthalene using 1- $\mu$ s excitation pulses

tendency of ionization potentials to decrease with increasing molecular size can be exploited to restrict detection to the larger species of interest. This behavior has already been established to be highly useful in one-photon photoionization detection. For the two-photon method, it will be possible to avoid interference from species with low ionization potentials if these species lack intermediate states of appropriate energies. An examination of one-photon absorption spectra and ionization potentials for PAH species leads to the conclusion that near UV laser sources will excite R2PI with high efficiency (approaching ionization of every molecule within the laser

interaction region). The cross sections for interfering processes such as two-photon resonance, three-photon ionization are lower by factors of  $\geq 10^4$  given typical laser powers. (The acetone peak in Figure 10 is an example of this type of three-photon interference.)

For practical application of R2PI it is relatively important to assess the effect of intermediate state lifetime on detection sensitivity. The overall rate of the R2PI process depends on this lifetime, provided ionization is slow with respect to the decay rate of the state. Therefore the relative R2PI responses for different compounds will depend upon the intensity and duration of the excitation pulse. The data represented by Figures 10a and 10b for naphthalene and its haloderivatives are representative for the range of excited state lifetimes likely to be encountered.

Considering that the fluorescence quantum yields for these compounds range from 0.18 for naphthalene to approximately  $10^{-4}$  for idonaphthalene and a similar trend applies to the  $S_1$  lifetimes, it is apparent that photoionization detection provides nearly uniform detection sensitivity when 5-ns excitation pulses are used. Therefore, either ionization occurs before significant relaxation of  $S_1$  occurs or the dissociation products formed from  $S_1$  ionize efficiently, provided sufficient excitation intensity is used. Response to compounds with short excited-state lifetimes is reduced substantially when 1- $\mu$ s excitation pulses are used (Figure 10b). The process is easily modeled for these two important cases: (1) excitation pulses of shorter duration than the excited state lifetimes and intensity low enough to avoid significant depletion of  $S_0$ , and (2) excitation pulses of much longer duration than the excited state lifetime, resulting in a steady-state population in  $S_1$  under conditions of low excitation intensity. In both cases, it has been assumed that molecular absorption transitions span the entire laser linewidth, a condition easily fulfilled by the PAH molecules of interest.

Assuming low intensity excitation pulses with rectangular temporal shape and duration  $\Delta t$ , the weak signal expression for the number of signal ions ( $N_i^1$ ) produced per short duration laser pulse is

$$N_i^1 = (A) n_0 \sigma_1 \sigma_2 I^2 (\Delta t^2 / 2) \quad (1)$$

where  $A$  is the cross sectional area of the excitation beam,  $l$  is the interaction length,  $n_0$  is the density of ground state molecules,  $\sigma_1$  is the one-photon absorption cross section for the transition from the ground state  $|0\rangle$  to the excited state  $|1\rangle$ ,  $\sigma_2$  is the photoionization cross section for state  $|1\rangle$ , and  $I$  is the intensity of the excitation beam. (It is assumed that states or species formed by decay of  $|1\rangle$  do not contribute.)

The corresponding expression for the number of ions  $N_i^1$  generated per pulse by a low power long duration rectangular pulse, case 2, is given by

$$N_i^1 = (A) n_0 \sigma_1 \sigma_2 I^2 \Delta t \tau \quad (2)$$

where  $\tau$  is the effective lifetime of the state being photoionized,  $|1\rangle$ . The ratio ( $R$ ) of signal for fast excitation vs. slow excitation, assuming pulses of equal energy and cross sectional area, is given by

$$R = \Delta t_1 / 2\tau \quad (3)$$

where  $\Delta t_1$  is the longer pulse duration. In this derivation, coherence effects have been neglected, which is justified by the high pressure conditions used for the measurements. These estimates are expected to provide a qualitative description of the process. It is clear that there are significant analytical advantages to short pulse excitation for multiphoton photoionization detection. Sensitivity decreases when the excitation pulse duration greatly exceeds the intermediate

state lifetime. Given an excitation source that produces pulses shorter than intermediate state relaxation times, the sensitivity becomes lifetime independent. For detection of species with unusually long intermediate state lifetimes, it will be possible to achieve added detection selectivity, without compromising sensitivity, by using long duration excitation pulses. Then, in accord with Equation 2, efficient ionization occurs for species with large lifetimes ( $\tau$ ) and ionization of other species with short lifetimes is less efficient.

The detection limit of 10 pg measured for anthracene was imposed by fluctuations in a background signal than can be attributed to impurities bleeding from the chromatographic column. The background decreases at low temperature and it is not observed in a pure stream of carrier gas. The most direct approach to reduce the background is to use a capillary column with an improved substrate. Alternative approaches involve using a more stable laser system or correcting for laser intensity fluctuations by measuring the ratio of the signal from a measurement column to the signal from a reference column on a pulse-to-pulse basis.

In an optimum chromatographic system, it should be possible to obtain detection limits comparable to  $5 \times 10^4$  molecules/cm<sup>3</sup> in the ionization cell, which was recently measured by R2PI in argon and in nitrogen buffer gases using an advanced laser source. For lasers comparable to those used in this study, it is possible to detect on the order  $10^7$  molecules/cm<sup>3</sup> in the ionization cell. On this basis, subfemtogram detection limits can be projected for aromatic hydrocarbons using advanced laser sources and detection of 1-10 femtograms should be possible with modest laser systems.

The small volume proportional counter used in these studies matches the small volumetric flow of capillary columns; however, the device has a range of linear response limited to about three decades. When larger concentrations of ions are present, space charge builds up in the region of the small anode and reduces proportional counter gain. This problem can be reduced substantially by increasing the effective anode wire length or by using a unit gain ionization cell which is linear over many decades and relying on an external amplification device with high gain. Using state-of-the-art amplification, currents corresponding to 100 electrons can be detected in a unit gain ionization cell. For many purposes, it is satisfactory to adjust the ion concentration to within the linear range by inserting calibrated attenuation filters into the excitation beam, provided the signal is normalized accordingly. In prior work, this procedure was used to extend an analytical curve over 8 decades of concentration. Therefore, substantial improvement in dynamic range can be expected for gas chromatographic applications.

## CONCLUSIONS

Resonance enhanced two-photon photoionization detection is easily interfaced to a conventional gas chromatograph column. A proportional counter is an ideal detector for this application in that it operates efficiently at ambient pressure in the oxygen-free carrier gas stream. The results for spectral discrimination between anthracene and phenanthrene are illustrative of what can be achieved in an ideal case. Two-photon ionization spectra are not widely available for other compounds; therefore, conclusions with respect to ability to achieve similar discrimination for other compounds must await additional studies. It is highly probable that a widely applicable discrimination capability can be achieved by using more sophisticated multiwavelength excitation methods and by adding time-of-flight ion mobility measurement. Discrimination of anthracene and phenanthrene has been demonstrated for illustrative purposes. Although it is possible to resolve these isomers by modern chromatographic techniques, it is difficult to resolve isomers of many heavier PAH species.

The R2PI method should be valuable for detection of these species.

The studies described in this report were not designed to establish the ultimate detection limits obtainable by R2PI in conjunction with gas chromatography. Nonetheless, detection of PAH compounds at levels down to 10 pg was easily achieved. Improvement by a factor of ten can be expected given state-of-the-art chromatographic technique and an additional factor of 100-1000 may be realized given an improved laser system.

#### ACKNOWLEDGMENT

The authors express their appreciation to Jerry Gelbwachs and Richard Keller for helpful suggestions concerning the manuscript.

#### LITERATURE CITED

- (1) Frusholtz, R.; Wessel, J.; Wheatley, E. *Anal. Chem.* **1980**, *52*, 281-284.
- (2) Brophy, J. H.; Rettner, C. T. *Opt. Lett.* **1979**, *4*, 337-339.
- (3) Brophy, J. H.; Rettner, C. T. *Chem. Phys. Lett.* **1979**, *67*, 351-355.
- (4) Antonov, V. S.; Kryazev, I. N.; Letokhov, V. S.; Matuk, V. M.; Movshev, V. G.; Potapov, V. K. *Opt. Lett.* **1978**, *3*, 37-39.
- (5) Heid, B.; Mainfray, G.; Manua, C.; Morellec, J.; *Phys. Rev. Lett.* **1972**, *28*, 130-131.
- (6) Lineberger, W. C.; Patterson, T. A. *Chem. Phys. Lett.* **1972**, *13*, 40-44.
- (7) Johnson, P. M.; Berman, M. R.; Zakheim, D. J. *J. Chem. Phys.* **1975**, *62*, 2800-2502.
- (8) Johnson, P. M. *J. Chem. Phys.* **1975**, *62*, 4562-4563.
- (9) Johnson, P. M. *J. Chem. Phys.* **1976**, *64*, 4638-4644.
- (10) Johnson, P. M. *Acc. Chem. Res.* **1980**, *13*, 20-26.
- (11) Petty, Gena; Tai, C.; Dalby, F. W. *Phys. Rev. Lett.* **1975**, *34*, 1207-1209.
- (12) Parker, D. H.; Sheng, S. I.; El-Sayed, M. A. *J. Chem. Phys.* **1976**, *65*, 5534-5535.
- (13) Parker, D. H.; Berg, J. O.; El-Sayed, M. A. *Chem. Phys. Lett.* **1978**, *56*, 197-199.
- (14) Berg, J. O.; Parker, D. H.; El-Sayed, M. A. *Chem. Phys. Lett.* **1978**, *56*, 411-413.
- (15) Parker, D. H.; El-Sayed, M. A. *Chem. Phys.* **1979**, *42*, 379-387.
- (16) Parker, D. H.; Pandolf, R.; Stannard, P. R.; El-Sayed, M. A. *Chem. Phys.* **1980**, *45*, 27-37.
- (17) Feldman, D. L.; Leng, R. K.; Zare, R. N. *Chem. Phys. Lett.* **1977**, *52*, 413-417.
- (18) Lubman, D. M.; Naaman, R.; Zare, R. N. *J. Chem. Phys.*, in press.
- (19) Herrmann, A.; Leutwyler, S.; Schumacher, E.; Woste, L. *Chem. Phys. Lett.* **1977**, *52*, 418-425.
- (20) Zandee, L.; Bernstein, R. B.; Lichtin, D. A. *J. Chem. Phys.* **1978**, *69*, 3427-3429.
- (21) Zandee, L.; Bernstein, R. B. *J. Chem. Phys.* **1979**, *70*, 2574-2575.
- (22) Krogh-Jespersen, K.; Rava, R. P.; Goodman, L. *Chem. Phys. Lett.* **1979**, *64*, 413-416.
- (23) Krogh-Jespersen, K.; Rava, R. P.; Goodman, L. *Chem. Phys.* **1979**, *44*, 295-302.
- (24) Williamson, A. D.; Compton, R. N. *Chem. Phys. Lett.* **1979**, *62*, 295-297.
- (25) Williamson, A. D.; Compton, R. N.; Eland, J. H. D. *J. Chem. Phys.* **1979**, *70*, 590-591.
- (26) Hurst, G. S.; Nayfeh, M. H.; Young, J. P. *Appl. Phys. Lett.* **1977**, *30*, 229-231.
- (27) Hurst, G. S.; Payne, M. G.; Kramer, S. D.; Young, J. P. *Rev. Mod. Phys.* **1979**, *51*, 767-819.
- (28) Driscoll, J. N.; Ford, J.; Jaramillo, L.; Becker, J. H.; Hewitt, G.; Marshall, J. K.; Onishuk, F. *Am. Lab.* **1978**, *10*(5), 137-147.
- (29) Driscoll, J. N.; Ford, J.; Jaramillo, L. F.; Gruber, E. T. *J. Chromatogr.* **1978**, *158*, 171-180.
- (30) Hansch, T. W. *Appl. Opt.* **1972**, *11*, 895.

RECEIVED for review January 21, 1980. Accepted April 8, 1980. This work was supported in part by the U.S. Air Force Office of Scientific Research under Grant AFOSR-77-3438, by the National Science Foundation under Grant CHE77-16074, and by the Department of Energy, Contract DE-ACO3-79EV10239.

## APPENDIX D

### Ion Dip Spectroscopy: A New Technique of Multiphoton Ionization Spectroscopy Applied to $I_2$

## **Ion Dip Spectroscopy: A New Technique of Multiphoton Ionization Spectroscopy Applied to $I_2$**

**Donald E. Cooper, Charles M. Klimcak, and John E. Wessel**  
*The Aerospace Corporation, Los Angeles, California 90009*  
(Received 17 October 1980)

A new method of high-resolution multiphoton spectroscopy based on competition between ionization and stimulated-emission channels is described. It combines features of multiphoton photoionization with those of optical-optical double resonance. Results obtained for  $I_2$  demonstrate the method and identify intermediate states involved in multiphoton photoionization. The method offers the potential for extremely sensitive sub-Doppler spectroscopy of complex molecules.

PACS numbers: 33.80.Kn, 07.65.Eh, 33.40.-e, 42.65.Gv

In this Letter, we describe and demonstrate a new two-wavelength method of multiphoton photoionization spectroscopy<sup>1</sup> (MPI) termed ion dip spectroscopy. Results are presented for application to multiphoton spectroscopy of the iodine

molecule.<sup>2,3</sup> Ion dip spectroscopy combines the extreme sensitivity of resonance-enhanced two-photon photoionization<sup>4</sup> with the high resolution of techniques such as coherent anti-Stokes Raman scattering (CARS), stimulated-Raman-gain spec-

troscopy, and stimulated-emission spectroscopy.<sup>3</sup> In analogy with related double-resonance techniques,<sup>6</sup> ion dip spectroscopy eliminates spectral congestion and permits assignment of intermediate states involved in MPI. It should furnish the high selectivity needed for detection and study of complex polyatomic species at concentrations approaching the single-molecule limit.

Consider the four-level system shown in Fig. 1 with ground state  $|0\rangle$ , excited vibrational level  $|v\rangle$ , excited electronic state  $|1\rangle$ , and ionized state  $|I\rangle$ . Two photons at  $\omega_1$  induce efficient ionization because resonance enhancement occurs through state  $|1\rangle$ . A high-intensity laser probe at frequency  $\omega_2 < \omega_1$  is introduced. When  $\omega_1 - \omega_2$  matches suitable ground-state vibrational frequencies, stimulated emission (stimulated Raman if  $\omega_1$  is out of resonance with  $|1\rangle - |0\rangle$ ) competes with ionization.<sup>7</sup> This decreases the effective population in  $|1\rangle$  and reduces the ionization signal, provided population inversion occurs between  $|1\rangle$  and  $|v\rangle$ . (Ion dips may also occur if  $|v\rangle$  is at higher energy than  $|1\rangle$ . Predissociative states should provide a highly efficient channel leading to loss of ionization.) The method can also be applied to MPI processes that require more than two  $\omega_1$  photons for ionization. We demonstrate the method with iodine by using five  $\omega_1$  photons to induce ionization and one  $\omega_2$  photon to stimulate the ion dip signal.

The experimental setup is illustrated in Fig. 2. A single Nd<sup>3+</sup>-doped yttrium aluminum garnet laser pumped two dye-laser-amplifier systems producing pulses of  $5 \times 10^{-9}$  s duration at a 10 Hz repetition rate. A grazing-incidence-configuration laser<sup>8</sup> provided low-power  $\omega_1$  pulses with energy of order  $3 \times 10^{-4}$  J and linewidth about  $0.2 \text{ cm}^{-1}$ . A Hansch-type dye laser<sup>9</sup> with a pressure-scanned intracavity etalon furnished the higher-

power  $\omega_2$  beam with energy of order  $3 \times 10^{-3}$  J/pulse and linewidth of order  $0.1 \text{ cm}^{-1}$ . Wavelengths were monitored to  $\pm 0.3 \text{ cm}^{-1}$  by an external spectrometer not shown in the figure. A differential measurement technique was employed in order to reduce noise associated with pulse-to-pulse variations in laser-excitation efficiency. One pair of electrodes measured ion current in the region where a gently focused  $\omega_1$  beam intersects the unfocused  $\omega_2$  beam. A second pair of electrodes measured ion current in a region where the  $\omega_1$  and  $\omega_2$  beams do not overlap. Output signals were applied to a differential amplifier, thereby eliminating the one-wavelength components of the signal derived from  $\omega_1$  alone and  $\omega_2$  alone. Output from the amplifier was sampled using a boxcar integrator with a  $10^{-6}$ -s gate width.

Figure 3 presents the one-wavelength  $I_2$  MPI spectrum obtained in this study and the corresponding portion of the high-resolution one-photon B-X absorption spectrum published by Simmons and Hougen.<sup>10</sup> The one-photon transition corresponds to excitation from  $v''=0$  in the ground state to  $v'=26$  in the B state.<sup>11</sup> Close spacing of rotational features in the one-photon spectrum [Fig. 3b] prevents individual transitions from being resolved with use of a  $0.2\text{-cm}^{-1}$  laser linewidth.

The MPI spectrum (which involves ionization by at least five photons) is simple in comparison. It is dominated by two distinct peaks at  $18393.9 \text{ cm}^{-1}$  and  $18395.1 \text{ cm}^{-1}$  that are ten times as intense as any other features in the region we have studied from  $18390$  to  $18403 \text{ cm}^{-1}$ . The apparent sparsity of the MPI spectrum arises from the requirement for multiple resonances between the highly excited states involved in the five-photon

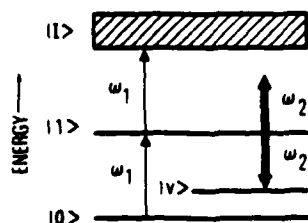


FIG. 1. Simplified energy-level diagram for ion dip spectroscopy. This scheme is appropriate for two-photon near-uv ionization of polyatomic molecules. For  $I_2$ , the B-state resonance corresponds to  $|2\rangle$  and higher-state resonances have been omitted from the diagram.

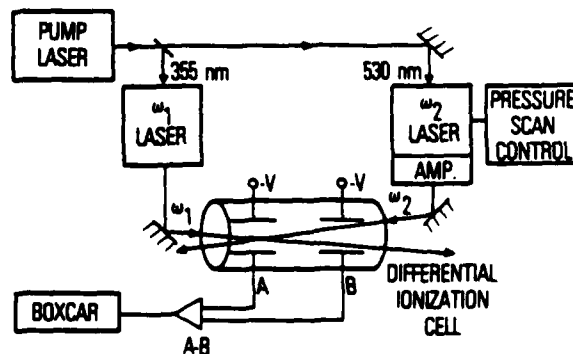


FIG. 2. Experimental setup with differential detection.



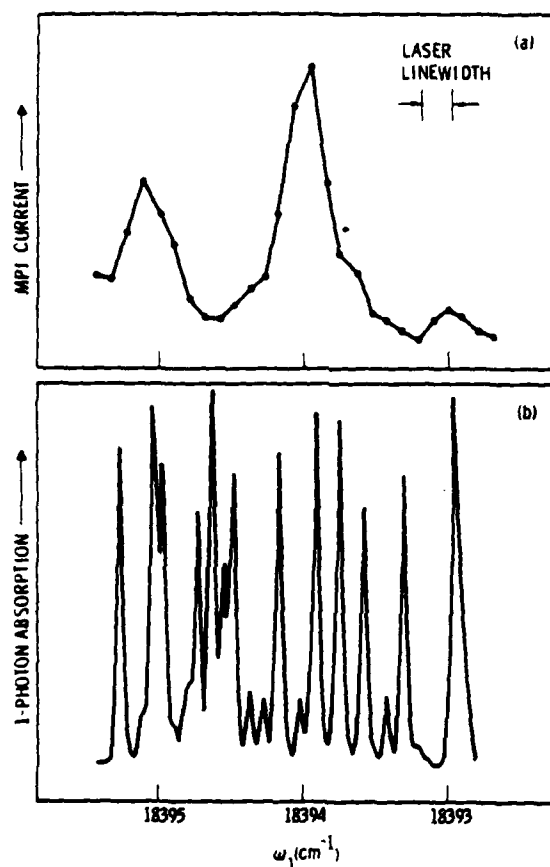


FIG. 3. Comparison of (a) MPI spectrum of  $\text{I}_2$  with (b) the absorption spectrum recorded in the region  $B(v'=26)-X(v''=0)$ . Note that the experimental spectra are subject to errors of  $\pm 0.3 \text{ cm}^{-1}$  from point to point. No correction has been applied to the one-photon spectrum for variations in fluorescence quantum yield.

ionization process. The spectra in Fig. 3 are consistent with this expectation; however, they do not demonstrate convincingly that  $B-X$  resonances are involved in the MPI process. Lehmann, Smolarek, and Goodman<sup>3</sup> studied MPI of  $\text{I}_2$  in adjacent spectral regions and also reported that it is difficult to identify correspondences between the MPI spectra and one-photon transitions of the complex  $B-X$  system.

Ion dip spectra readily identify resonances involved in the one-wavelength MPI spectrum of Fig. 3. In the presence of  $\omega_1$  set at the MPI peak at  $18393.9 \text{ cm}^{-1}$ , a second laser induced spectrally sharp dips ( $\Delta\omega < 0.2 \text{ cm}^{-1}$ ) in the ionization current at  $\omega_2 = 14941.5 \text{ cm}^{-1}$  and at  $\omega_2 = 14938.1 \text{ cm}^{-1}$ . These  $\omega_2$  transitions are readily assigned

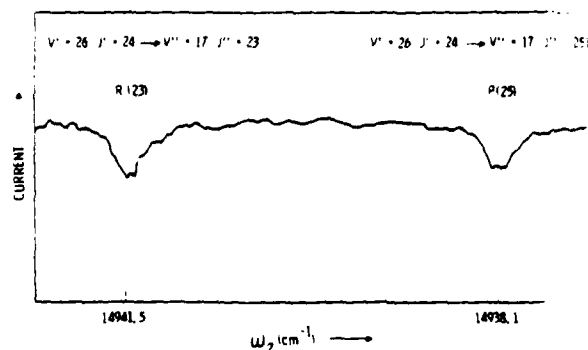


FIG. 4. Ionization dip spectrum recorded with  $\omega_1 = 18393.9 \text{ cm}^{-1}$ .

to R(23) and P(25) of  $B(v'=26)-X(v''=17)$ . Similar dips were observed for transitions  $v' = 26, j' = 15, 14$ . Representative spectra are reproduced in Fig. 4. Failure to observe dips for  $v' = 26, j' = 16$  is consistent with the small Franck-Condon factor for this transition. A second set of ion dips, corresponding to R(15) and P(17), was observed for  $v' = 26, j' = 15, 14$  ( $v'' = 17$  was not investigated) when the  $\omega_1$  laser was tuned into resonance with the second strong MPI feature at  $18395.1 \text{ cm}^{-1}$ . For all transitions the measured positions are within  $\pm 0.3 \text{ cm}^{-1}$  of the accurately known  $B-X$  transition energies<sup>11</sup> and P to R branch intervals are within  $\pm 0.2 \text{ cm}^{-1}$  of calculated values. Thus the ion dip technique allows assignment of specific intermediate states in an MPI spectrum. The simplicity of the ion dip

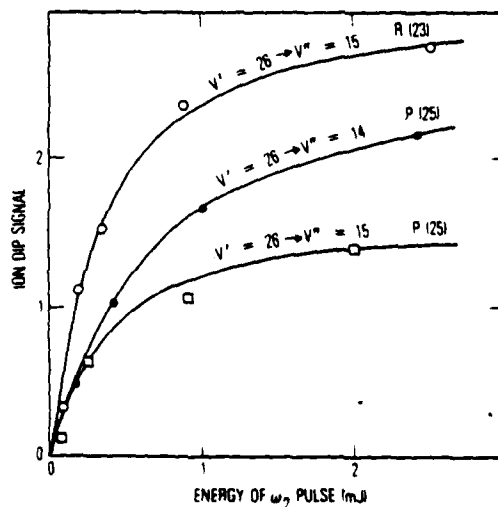


FIG. 5. Optical-saturation curves obtained by varying neutral density in the  $\omega_2$  beam.

spectra indicates that each MPI peak involves a single rovibronic state in the  $B$  electronic state.

The ion dip transition amplitude (measured in arbitrary units corresponding to the reduction in current from the value obtained with nonoverlapping  $\omega_1$  and  $\omega_2$  beams) is shown as a function of the intensity of the  $\omega_2$  beam in Fig. 5. Observed data points for three separate transitions are well represented by the expected functional form (solid lines) for optical saturation of a two-level system ( $|1\rangle - |0\rangle$ ). Saturation intensities (at which the ion dip has reached one-half its maximum amplitude) extracted from the data are within experimental error limits of the theoretical values derived from known Franck-Condon factors<sup>12</sup> and  $B$ -state lifetimes.<sup>13</sup> For the largest ion dips, the MPI signal declines to about two-thirds the current obtained with  $\omega_1$  alone. This is consistent with the expectation that population will be approximately equilibrated between states  $|0\rangle$ ,  $|1\rangle$ , and  $|v\rangle$  under strong pumping conditions. Production of larger ion dips would require the use of coherent excitation conditions whereby  $\pi$  pulses would transfer all population in level  $|1\rangle$  into level  $|v\rangle$ . Close agreement between the observed saturation data and the incoherent two-level model of saturation is obtained because the laser linewidth exceeds the Doppler width and because the  $\omega_1$  beam probes a region of relatively constant intensity in the larger  $\omega_2$  beam.

Ion dip spectroscopy is not limited to study of  $B-X$  transitions. Iodine has a rich spectrum of electronic states<sup>14</sup> above the  $B$  state which clearly plays a role in the MPI spectrum. We have observed numerous ion dip features arising from upward transitions induced by  $\omega_2$  from the  $B$  state to a new weakly bound state. Observed vibrational intervals and  $P$  to  $R$  splittings in the ion dip spectra yield extensive information about the shape and position of the potential curve of this upper state. These transitions will be reported in detail at a later time. In addition to the ion dip spectra, we have observed a large number of transitions in which the ionization signal is enhanced by the combined presence of  $\omega_1$  and  $\omega_2$ . These transitions involve resonances between highly excited states occurring at  $\omega_1$ . It is anticipated that upward transitions to dissociative states will also be observed and that the spectra should reveal intensity modulation arising from Condon diffraction.<sup>15</sup>

Based on prior MPI work<sup>1,4</sup> with organic compounds, ion dip spectroscopy should be widely applicable to polyatomic species and detection

limits in the range of  $10^2$  molecules/cm<sup>3</sup> can be anticipated. The ability to simplify the congested spectra of large polyatomic species by isolating MPI transitions involving individual rotational levels of the ground electronic state will be particularly valuable for detection of large polyatomic species at low concentrations because these molecules generally have severely overlapping rovibronic transitions. In spectroscopic applications the high sensitivity, combined with Doppler-free resolution and the ability to identify specific MPI channels, will make this technique a valuable new tool. Additional experimental refinements may be advantageous. For example, the amplitude of the ion dip signal could be increased by using a time-delayed  $\pi$  pulse for  $\omega_2$ . A third low-intensity ionizing pulse at  $\omega_3$ , delayed with respect to  $\omega_2$ , would probe for complete depopulation of  $|2\rangle$ . For applications demanding maximum resolution,<sup>16</sup> concurrent  $\omega_1$  and  $\omega_2$  beams would be used and the intensities of both beams would be minimized.

This research was supported by the U. S. Air Force Office of Scientific Research under Grant No. AFOSR-77-3438, the Department of Energy, Office of the Environment, under Contract No. DE-AC03-79EV10239, and the National Science Foundation under Grant No. CHE-77-16074. The authors would like to acknowledge helpful discussions with Dr. Jerry Gelbwachs.

<sup>1</sup>P. Johnson, *Acc. Chem. Res.* **13**, 20 (1980).

<sup>2</sup>G. Petty, C. Tai, and F. Dalby, *Phys. Rev. Lett.* **34**, 1207 (1975); F. W. Dalby, G. Petty-Sil, M. H. L. Petty-Sil, and C. Tai, *Can. J. Phys.* **55**, 1033 (1977).

<sup>3</sup>K. Lehman, J. Smolarek, and L. Goodman, *J. Chem. Phys.* **69**, 1569 (1978).

<sup>4</sup>C. Klimcak and J. Wessel, *Appl. Phys. Lett.* **37**, 138 (1980).

<sup>5</sup>A. Owyong, *IEEE J. Quant. Electron.* **14**, 192 (1978); J. B. Koffend, R. Bacis, and R. W. Field, *J. Chem. Phys.* **70**, 2366 (1979).

<sup>6</sup>C. Wieman and T. W. Hansch, *Phys. Rev. Lett.* **36**, 1170 (1976); R. W. Field, G. A. Capelle, and M. A. Revelli, *J. Chem. Phys.* **63**, 3228 (1975); M. E. Kaminsky, R. T. Hawkins, F. V. Kowalski, and A. L. Schawlow, *Phys. Rev. Lett.* **36**, 671 (1976); F. V. Kowalski, W. T. Hill, and A. L. Schawlow, *Opt. Lett.* **2**, 112 (1978); P. J. Domaille, T. C. Steimle, and D. O. Harris, *J. Chem. Phys.* **68**, 4977 (1978).

<sup>7</sup>For molecules, excited-state ionization cross sections are expected to be comparable to cross sections for the bound transitions such as  $|1\rangle - |0\rangle$ . Therefore

the intensity at  $\omega_1$  should generally be maintained less than that at  $\omega_2$ , otherwise (1) will be irreversibly depopulated by ionization prior to downpumping by the  $\omega_2$  beam and the ion dip signal will be correspondingly reduced.

<sup>8</sup>I. Shoshan, N. N. Danon, and U. P. Oppenheim, *J. Appl. Phys.* **48**, 4495 (1977); M. G. Littman and H. J. Metcalf, *Appl. Opt.* **17**, 224 (1978); M. G. Littman, *Opt. Lett.* **3**, 138 (1978).

<sup>9</sup>T. W. Hansch, *Appl. Opt.* **11**, 895 (1972).

<sup>10</sup>J. D. Simmons and J. T. Hougén, *J. Res. Nat. Bur. Stand.* **81A**, 25 (1977).

<sup>11</sup>R. F. Barrow and K. K. Yee, *J. Chem. Soc. Faraday Trans. 2* **69**, 684 (1973); R. J. LeRoy, *J. Chem. Phys.*

**52**, 2683 (1970).

<sup>12</sup>K. K. Yee, unpublished.

<sup>13</sup>G. A. Capelle and H. P. Broida, *J. Chem. Phys.* **58**, 4212 (1973).

<sup>14</sup>R. S. Mulliken, *J. Chem. Phys.* **55**, 288 (1971).

<sup>15</sup>E. U. Condon, *Phys. Rev.* **32**, 858 (1928); R. S. Mulliken, *J. Chem. Phys.* **55**, 309 (1971); D. L. Rousseau and P. F. Williams, *Phys. Rev. Lett.* **33**, 1368 (1974); J. Tellinghuisen, *Phys. Rev. Lett.* **34**, 1137 (1975).

<sup>16</sup>Low intensity would be required in order to avoid power broadening and ac Stark shifts, and low-pressure conditions would be necessary to avoid pressure and high-resolution conditions.